

APPLICATION OF SWAT-MODFLOW SOFTWARE TO EVALUATE GROUNDWATER-  
SURFACE WATER INTERACTION IN WEST-CENTRAL ALBERTA

by

David Chunn

A thesis submitted in partial fulfillment of the requirements for the degree of

Master of Science

Department of Earth and Atmospheric Sciences  
University of Alberta

© David Chunn, 2018

## **Abstract**

Responsible watershed management is emerging as a key issue as humanity continues to place increasing demands on water resources. To meet future demands, it has become imperative that water resources be managed as a holistic system rather than solely focusing on individual aspects. Hydro(geo)logic models are one tool that can aid in understanding the complex factors that control water supply and management. Historically, hydro(geo)logic models have focused on either surface water or groundwater processes separately. However, there has been a recent push to develop models that consider both systems. This study applies a coupled surface water-groundwater (SW-GW) tool, SWAT-MODFLOW, to the Little Smoky River watershed in the Fox Creek area of Alberta, Canada in order to study the dynamics of a water supply and demand system in an area of high industrial activity. The coupled model integrates hydro(geo)logical processes of physical flow, providing a more accurate representation of the dynamic relationships between natural and anthropogenic factors that control the SW and GW of the region's flow system.

The primary objective of this study is to test SWAT-MODFLOW's ability to simulate a more complex and variable region, as previous studies had a greater focus on the surface system's interaction with shallow groundwater aquifers in smaller watersheds, and in more temperate climates. To that end, the model used in this project includes seven layers in MODFLOW that correspond to geologic formations, ranging widely in terms of their thicknesses and hydraulic properties. The model was subjected to snow and climate change influence, and each component model (SWAT and MODFLOW) was built and calibrated separately during the study. The result was a coupled tool that successfully included new influences, widening the possible range of scenarios in which this tool can be applied.

## **Acknowledgements**

I would like to start by thanking both of my supervisors, Dr. Daniel Alessi and Dr. Monireh Faramarzi, for providing me with this fantastic study opportunity, as well as their guidance throughout its course. Each supervisor offered experiences that caused paradigm shifts for me as a professional and as a lifelong learner. With their combined efforts, the scale and impact of this work grew beyond what I could have imagined.

In addition, the contributions of Brian Smerdon of the Alberta Geological Survey were paramount to the study's success. The importance of the discussions, data and advice given for the benefit of the study cannot be overstated.

I would also like to thank the organizations that provided funding for this research. NSERC, Encana and CAIP contributed funding to the lab groups of Dr. Daniel Alessi and Dr. Monireh Faramarzi, and Alberta Scholarships provided the Alberta Graduate Student Scholarship and the Queen Elizabeth II Graduate Scholarship, which directly funded the study.

This work also could not have been done without the endless support of my amazing parents, brother, girlfriend and friends. They are always willing to listen, offer kind words and help to relieve the stress that naturally comes with an undertaking such as this. I speak the truth when I say that I could not have done this without you.

# TABLE OF CONTENTS

<b>1. INTRODUCTION</b> .....	1
1.1 – Water-Food-Energy Nexus.....	1
1.2 – The WFE and Hydraulic Stimulation Operations.....	3
1.3 – The WFE Nexus’ Relation to Modelling.....	5
1.4 – Case Study: Fox Creek Area.....	10
1.5 – Component Model Overviews and Previous Work.....	11
1.5.1. <i>SWAT: Overview</i> .....	11
1.5.2. <i>MODFLOW: Overview</i> .....	13
1.5.3. <i>Previous Work</i> .....	15
1.6 – Objectives and Hypotheses.....	22
1.6.1. <i>Gaps in Knowledge</i> .....	22
1.6.2. <i>Study Goals</i> .....	23
1.6.3. <i>Hypotheses</i> .....	24
<b>2. METHODS</b> .....	26
2.1 – Study Area.....	26
2.1.1. <i>Surface Hydrology</i> .....	27
2.1.2. <i>Geology and Hydrogeology</i> .....	29
2.2 – Model Development and Input Data .....	33
2.2.1. <i>SWAT Model Development</i> .....	33
2.2.2. <i>MODFLOW Model Development</i> .....	37
2.2.3. <i>SWAT-MODFLOW Integration</i> .....	40
2.3 – Calibration, Validation and Uncertainty Analysis.....	43
2.3.1. <i>Importance of Calibration</i> .....	43
2.3.2. <i>SWAT Calibration</i> .....	44
2.3.3. <i>MODFLOW Calibration</i> .....	47
2.4 – Scenario Analysis.....	50
<b>3. RESULTS AND DISCUSSION</b> .....	54
3.1 – Parameter Sensitivity Results.....	54
3.1.1. <i>SWAT</i> .....	54

3.1.2. <i>MODFLOW</i> .....	57
3.2 – SWAT-MODFLOW Runs and Results.....	61
3.2.1. <i>Results and Outputs</i> .....	61
3.2.2. <i>Streamflow and GW-SW Exchange</i> .....	62
3.2.3. <i>GW-SW Interaction Patterns</i> .....	66
3.2.4. <i>Model Outputs Discussion</i> .....	66
3.2.5. <i>Model Application: Water-Food-Energy Nexus</i> .....	67
3.3 – SWAT-MODFLOW as a GW-SW Tool.....	73
3.3.1. <i>Watershed and Scenario Simulation</i> .....	73
3.3.2. <i>Computational Time</i> .....	74
3.4 – Limitations.....	75
3.4.1. <i>Limitations: SWAT</i> .....	75
3.4.2. <i>Limitations: MODFLOW</i> .....	75
3.4.3. <i>Limitations: SWAT-MODFLOW</i> .....	77
3.5 – Future Research Directions.....	79
<b>5. CONCLUSION</b> .....	<b>80</b>
<b>6. REFERENCES</b> .....	<b>82</b>
<b>7. APPENDIX</b> .....	<b>92</b>

## List of Figures

Figure 1: The Water-Food-Energy (WFE) nexus, illustrating the interrelated nature of water resources. (adapted from Hoff, 2011).....	2
Figure 2: Conceptual diagram of the SWAT-MODFLOW model, outlining the component models responsible for each physical process (modified from Park and Bailey, 2017).....	7
Figure 3: Schematic of the hydrological cycle as represented by the SWAT model (modified from Neitsch et al., 2009).....	12
Figure 4: A diagram of box-centered flow, representative of how MODFLOW performs calculations. The Finite-Difference equation is evaluated at nodes located in the center of each cell, in three dimensions, determining flux in and out.....	14
Figure 5: The study area shown within the province of Alberta, Canada.....	26
Figure 6: Average temperature and precipitation graphs, taken at the Fox Creek Junction Station, Alberta (modified from The Weather Network, 2018).....	29
Figure 7: Representative stratigraphic column for West-Central Alberta (modified from AGS, 2015).....	30
Figure 8: (A) shows the Little Smoky River watershed (outlined in orange), displaying the study's delineated subbasins, and (B) displays the area's varying elevation.....	34
Figure 9: (A) shows the Little Smoky River's soil types, and (B) displays the land use types...	35
Figure 10: South-north cross-section of the MODFLOW modelled area, displaying the geological units present.....	38
Figure 11: Schematic of the SWAT-MODFLOW integration process, with the necessary steps and input files outlined (adapted from Park and Bailey, 2017).....	41
Figure 12: A colored contour map of hydraulic head for the Little Smoky River watershed, produced by Visual MODFLOW.....	49
Figure 13: Diagram of carbon dioxide concentrations when considered under various climate change scenarios, including RCP2.6 and RCP8.5 (adapted from van Vuuren et al., 2011).....	52
Figure 14: 95ppu graphs for both calibration points in the Little Smoky River Watershed over the entire historical simulation period.....	55-56
Figure 15: 3-D diagram of the study's MODFLOW model, with each color representing the hydraulic conductivity found at that point.....	58

Figure 16: Calibration graph for the MODFLOW component, comparing simulated hydraulic head values to the observed hydraulic head values at each observation well..... 60

Figure 17: Simulated vs. observed streamflow for the watershed’s two stream gauges (Flow\_119\_1 (A) and Flow\_118\_24 (B))..... 62

Figure 18: Plan view map of the Little Smoky River watershed, with long-term (1986-2007) average annual GW-SW exchanges displayed for each MODFLOW river grid cell..... 64

Figure 19: Long-term (1986-2007) average monthly GW-SW exchange differences from the overall (Figure 18) for each MODFLOW river cell, in the months of January (A), June (B), and October (C)..... 65

Figure 20: Map of the Little Smoky River watershed within the MODFLOW modelled area, with simulated pumping well locations included..... 68

Figure 21: Plan view map of the Little Smoky River watershed, with GW-SW exchanges displayed for each MODFLOW river grid cell. Pumping wells that have been installed within and proximal to the study area extract water at a rate of 468 m<sup>3</sup>/d, for six months of each simulation year..... 70

Figure 22: Projected long-term (2010-2034) average annual GW-SW exchanges under two simulation scenarios. (A) solely shows the effects of climate change, and (B) also includes a water well pumping rate of 4680 m<sup>3</sup>/d (pumping wells are the same as in Figures 20 and 21)... 72

## List of Tables and Workflows

Table 1: General information of selected GCMs and scenarios available from PCIC.....	53
Table 2: Final combined summary statistics for the calibrated and validated SWAT model. Initial refers to prior to calibration.....	57
Table 3: Summary statistics for the MODFLOW component. Although similar graphs can be displayed throughout the simulation period, the Normalized RMS remains relatively constant between 6% and 7%.....	60
Table 4: List of SWAT-MODFLOW outputs and their contents (modified from Beets, 2016).....	61
Table A1: List of major developments in SWAT-MODFLOW use, with alternative tools also listed.....	92
Table A2: Data sources for the study’s SWAT and MODFLOW component models.....	93
Table A3: Weather gauges near the Little Smoky River, with example average humidity and wind speed data for 2018 (modified from Alberta Agriculture and Forestry, 2018).....	95-96
Table A4: List of definitions for all parameters used in the SWAT-CUP calibration process (definitions based on Abbaspour, 2015).....	96-98
Workflow A1: Complete process of exporting river data from a SWAT model to create a .RIV boundary for a MODFLOW model.....	94
Workflow A2: Complete process of creating a .RCH file from the output of a SWAT model to import into the project’s MODFLOW model.....	94-95

# 1. INTRODUCTION

## 1.1. The Water-Food-Energy Nexus

Water is perhaps the most important element for the survival of life on Earth. Not only do humans need it at a biological level, but it is an essential component of nearly all industrial, agricultural and domestic activity worldwide. Global climate change will result in changes in local opportunities in water supply for these sectors (Alberta Water Portal Society, 2017).

Although food production and domestic water use have universal demand, petroleum extraction is a major industrial activity in many regions of the world that plays a pivotal role in stimulating the economy on provincial and national scales. While this contributes significantly to the annual Gross Domestic Product (GDP) of the countries in which it is produced, it is often strongly dependent on the availability and reliability of freshwater resources (Alessi et al., 2017; Faramarzi et al., 2017). The majority of contemporary works on water resources agree that the demands of various water-related sectors are interconnected (Bizikova et al., 2013). Due to their direct effects on human populations, and the economic success of countries, the food/agricultural and energy industries are commonly observed in close association with water and one another, and collectively referred to as the 'Water-Food-Energy (WFE) nexus' (Bizikova et al., 2013; Faramarzi et al., 2017; Waughray, 2011). Proper water management is emerging as a key challenge to the human race. Indeed, there are already indicators that anthropogenic influence is affecting the flow rates of rivers, as well as the winter recovery of glaciers (St. Jacques et al., 2010). As part of Waughray's (2011) book on the Water-Food-Energy nexus, McKinsey & Company compiled a group of statistics and forecasts for global water use in various sectors:

- Agriculture is the primary consumer of water worldwide, at 71% of global water withdrawals.

- Industrial activity (energy, manufacturing, etc.) currently accounts for 16% of global water withdrawals, but this is forecasted to grow to 22% by 2030.
- Domestic water withdrawals are projected to decrease as a total percentage (14% to 12%), but total volumetric demand will increase, especially in growing urban areas.

In effect, this means that even as relative water withdrawals in these sectors change, the overall global volume of extracted water is projected to increase, especially as factors such as population growth and improvements to quality of life come into play. The interrelated nature of these sectors is illustrated in Figure 1 (Hoff, 2011).

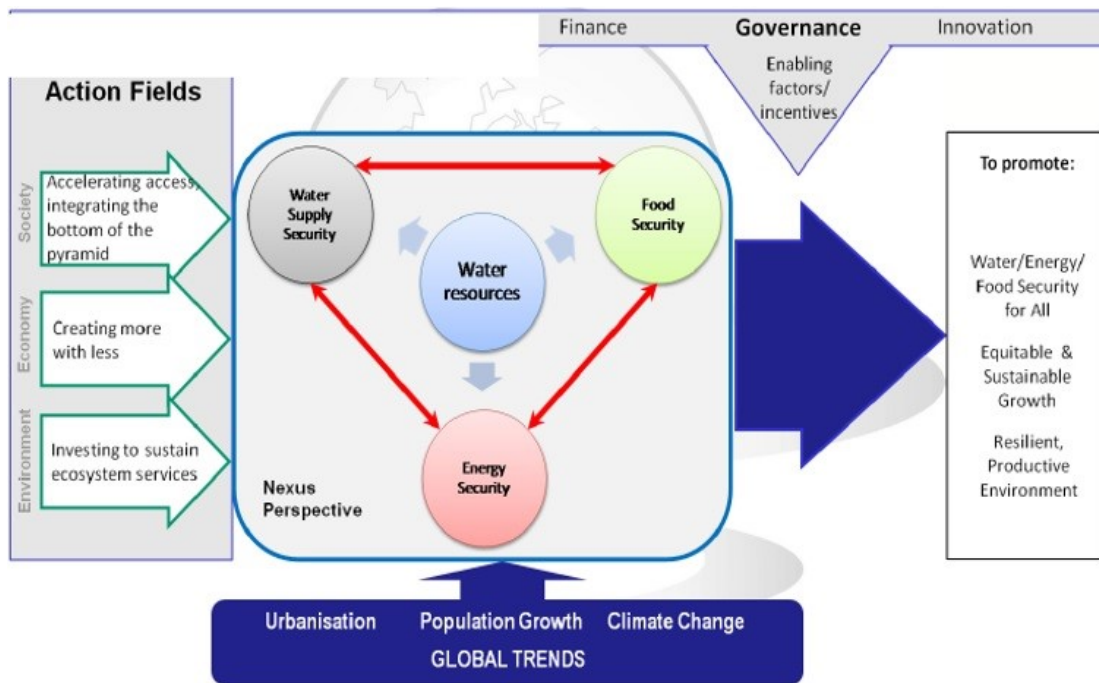


**Figure 1: The Water-Food-Energy (WFE) nexus, illustrating the interrelated nature of water resources. Factors such as population growth increase the demand and stress on each of the primary sectors described here (adapted from Hoff, 2011).**

In the United States and Canada, increasing energy production means that companies will require more access to water resources to fuel advanced extraction methods such as hydraulic stimulation and steam-assisted gravity drainage (Waughray, 2011; Johnson and Johnson, 2012). Historically, this has mainly meant extraction from freshwater sources such as lakes and rivers, but groundwater is seeing increased use as well (van der Gun, 2012; Hughes et al., 2017). When the water needs of the energy sector are combined with the needs of other sectors, it becomes clear that water must be managed systematically in order to ensure a sustainable supply for the future.

In theory, the global demand for water could be met through resource redistribution. The concept of “virtual water”, where consumer goods, energy and food products are compared to the amount of water it takes to produce them, has the potential to even the scales between water-scarce countries and water-rich countries (Yang and Zehnder, 2007). If water-scarce countries import food and energy from water-rich countries, it results in more local water being saved (Yang and Zehnder, 2007). As such, it is important for quantification of water and its uses at local and regional scales to occur. However, it is more difficult to put into practice, as the concept itself continues to be heavily debated (Horlemann and Neubert, 2006).

## **1.2. The WFE Nexus and Hydraulic Stimulation Operations**

Though the technology has existed for decades (Kerver, 1963), hydraulic stimulation (or hydraulic fracturing) has come into common use in the 21<sup>st</sup> century to increase oil and gas recovery from wells, especially for deep reservoirs with low porosity and permeability that require horizontal drilling. By injecting fracturing fluid into petroleum-rich bedrock reservoirs at high pressures, large fractures are formed in the target formation, which increases the flow of oil and/or gas into the well. Generally performed in multiple stages, starting from the furthest point

downhole and moving closer to the well's kickoff point (Alessi et al, 2017), this method of petroleum extraction has seen much success and is implemented in a multitude of oil and gas fields the world over.

Although other chemicals and solids are included in frac fluids, water is the principal ingredient, and as such must be extracted in large quantities for a successful hydraulic stimulation operation. The exact quantities, however, depend heavily upon the stimulation method used, the type of geologic formation being drilled, as well as project budgets (Johnson and Johnson, 2012; Alessi et al, 2017). A challenge in each of these operations (beside maximizing petroleum production) is maximizing the flow of return water, which is the water used for formation stimulation that returns to the surface. This, in turn, can be reused for further stimulation, which can lessen the project's environmental footprint and enhance its economic value (Paktinat et al., 2011). The different types of hydraulic stimulation techniques have varying return water rates, ranging from under 30% to 70% depending on the technique used (Johnson and Johnson, 2012). Additionally, the increasing number of fracture stages in these operations (Johnson and Johnson, 2012) means that the quantity of water used per well is also increasing.

Regardless of where oil and gas operations occur, a key component of any business plan is compliance with the environmental regulations of the area, usually controlled by provincial/state and/or federal Ministries associated with the government. This means that producers and operators must respect the boundaries set that protect everything from surface water and groundwater to plants, animals and air quality (CSUG, 2016). Depending heavily on the region, the regulations set around oil and gas operations (including hydraulic fracturing) vary widely. Alberta's are governed by the AER (Alberta Energy Regulator), which has detailed directives for all stages of a production cycle (AER, 2017). Due to the high industrial activity in the province,

Alberta's regulations around drilling and hydraulic fracturing are quite extensive (Notte et al., 2017); yet, there are still many areas that have room for improvement. One such example is the sourcing of water for hydraulic stimulation operations. A significant portion is extracted from local rivers and lakes, resulting in repercussions and complaints from domestic communities in the area. Though regulations concerning water extraction have historically been relatively lax, more strict regulations concerning these water bodies have emerged in recent years in response to communities near areas of heavy industry activity, such as Fox Creek (AER Bulletin 2015-25). As such, upstream producers and midstream operators are considering alternative sources, such as groundwater aquifers. Depending on the depth of the aquifers and levels of interaction with the surface systems, this may or may not be plausible.

### **1.3. The WFE Nexus' Relation to Modelling**

Much work must be done globally (and at all levels) to manage limited water resources to meet the increasing water demands of every sector. Eco-hydro-geologic modelling can be useful in quantifying the resources and needs of specific areas and understanding the natural and anthropogenic factors affecting their distribution in time and space (Faramarzi et al., 2015; Bailey et al., 2016; Masud et al., 2018). Depending on the scope of the research studies, models can be applied to regions of hugely varying size and complexity. As Bizikova et al. (2013) mention, it is important to develop holistic management strategies that relate many aspects of the Water-Food-Energy Nexus (and beyond) together. In light of this, computer models that quantify water resources should be holistic as well, focusing on groundwater (GW) and surface water (SW) together instead of treating them individually. Developing models that can accurately and consistently achieve this is a key step toward more intelligent water management.

The number of models that consider GW and SW together is continuously increasing. Therefore, considerations must be made during the selection process to ensure that the model is able to meet the demands of the study, including data availability, ease of use, accuracy of simulations and budget. Of those available, three coupled GW-SW tools have been used in multiple published basin-scale studies. These include HydroGeoSphere (Sudicky et al., 2008), GSFLOW (Markstrom et al., 2008) and SWAT-MODFLOW (Sophocleous et al., 1999; Kim et al., 2008., Guzman et al., 2015; Bailey et al., 2016).

Perhaps the best known of the available SW-GW technologies, Aquanty's HydroGeoSphere (HGS) (Sudicky et al., 2008) is a three-dimensional, finite-element numerical model with an unstructured grid. Based on the FRAC3DVS code developed by Therrien (1992), HGS began by simply simulating variably saturated GW flow and solute transport, with other modules such as surface water flow added on over time. The strength that HGS holds over most other integrated tools available today is that it considers both GW and SW flow together from the beginning of each project. This does away with the historical need to couple two separate codes, which benefits the overall representation of a user's conceptual model. Akin to other integrated models, it incorporates natural physical processes such as snowmelt and evapotranspiration, and also features the ability to simulate geologic media having fractures and macro-pores. Among the modules currently available, HGS is possibly the most powerful fully integrated SW-GW tool available, and can be applied to areas of hugely varying scale, from site-specific projects to river basin-wide studies (Aquanty, 2018). However, this power comes at a price – both literally and in terms of its computational burden. HGS can slow single-core computers down substantially, often requiring a high-powered machine to effectively carry out model runs (Brunner and Simmons, 2012). In addition, the incredible detail that HGS is capable of also demands sufficient

data in order for the model to maintain its superiority over other choices. Simulations may also take long periods of time, preventing calibration/parameter estimation from occurring to the same extent as in other models.

Born out of a need to track the interaction between SW and GW systems, SWAT-MODFLOW is a coupled hydro(geo)logical model that employs both SWAT and MODFLOW (SW and GW models, respectively – described further in Section 1.5) to yield an integrated output. Coupling the component models, SWAT and MODFLOW, helps to cover the limitations inherent in each code to yield a solution that is more faithful to real-world hydrology. As shown in Figure 2, SWAT covers the processes associated with SW hydrology, such as precipitation, temperature, stream flow, surface runoff, soil water, actual evapotranspiration and GW recharge (Eq. 1). On the other hand, MODFLOW is responsible for the GW processes in the study's watershed, including saturated flow and GW discharge into streams.

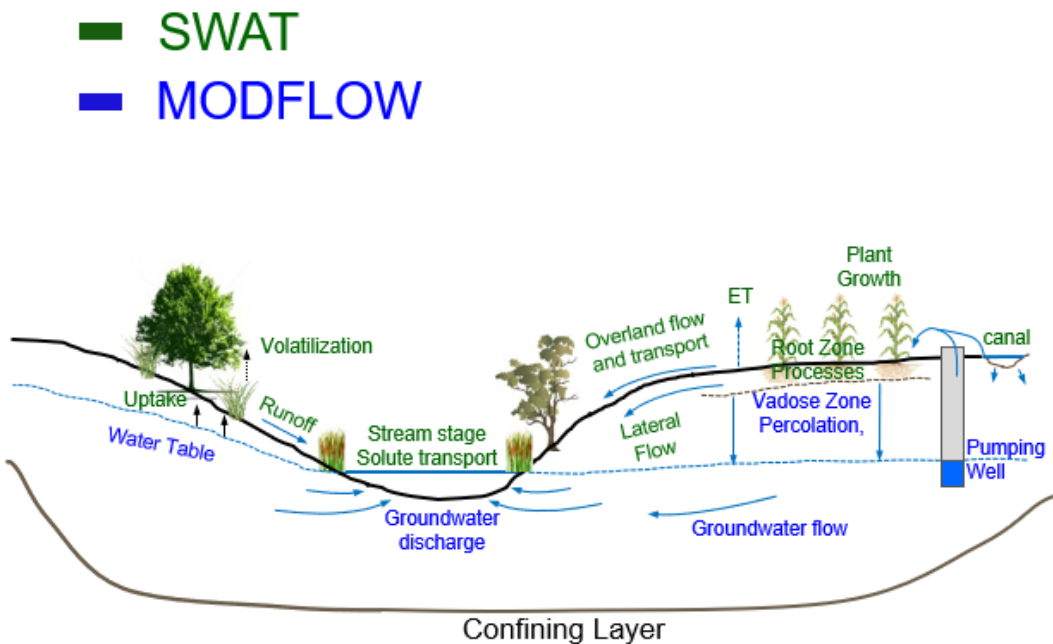


**Figure 2: Conceptual diagram of the SWAT-MODFLOW model, outlining the component models responsible for each physical process (modified from Park and Bailey, 2017).**

Although multiple SWAT-MODFLOW codes have been developed over the past twenty years for study areas of highly varying scale (Sophocleous et al., 1999; Kim et al., 2004a, b, 2008; Guzman et al., 2015; Bailey et al., 2016), each study was carried out to overcome the shortcomings of each of its component models (SWAT and MODFLOW), and to evaluate SW and GW resources as one system to achieve various goals (outlined below). While SWAT simulates physical processes associated with soil, plants, water in the root zone and weather, MODFLOW is responsible for providing outputs for three-dimensional GW flow, as well as well pumping simulations. Each SWAT-MODFLOW code follows the same general logic, in that MODFLOW is run as a subroutine of SWAT (Kim et al., 2008; Guzman et al., 2015; Bailey et al., 2016), effectively replacing SWAT's own GW module to yield more dynamic and detailed results for a given time step.

GSFLOW is an integrated SW-GW model developed by the USGS (United States Geological Survey) (Markstrom et al., 2008), and similar to SWAT-MODFLOW, simulates coupled hydrological flow. It uses MODFLOW for GW flow, and a USGS software called PRMS (Precipitation-Runoff Modeling System) (Leavesley et al., 1983) for SW flow. Although initial versions of this coupled model used MODFLOW-2005 as a GW engine, more recent versions employ MODFLOW-NWT, similar to the model used in this study (Ely and Kahle, 2012). A point of difference from SWAT-MODFLOW, however, is that MODFLOW is the component model primarily responsible for the simulation of water bodies such as rivers and lakes.

Similar to SWAT, PRMS functions with SW flow and climate data, and performs numerical calculations with the Hydrological Response Unit (HRU) method. This results in several HRUs

being delineated for a single watershed to accurately simulate the area's hydrology (Markstrom et al., 2008). Unlike SWAT-MODFLOW, however, GSFLOW's coding allows for simulations to be run in three ways: coupled, PRMS-only, or MODFLOW-only, which in turn permits more flexibility when calibrating the model.

GSFLOW's PRMS component has similar limitations to SWAT, in that it is discretized by HRU (Markstrom et al., 2008). This results in a more homogeneous representation of the real world than is normally desirable, as dominant properties for soil, land use, etc. are scaled up to represent a larger area (Bailey et al., 2016), thus potentially limiting its use for detailed analysis of the local processes in smaller-scale study areas. The limitations of MODFLOW in the context of GSFLOW are largely identical to those found in SWAT-MODFLOW (explained further in Section 1.5), as the engine used (MODFLOW-NWT) is the same. However, some additional complications may arise from MODFLOW being the primary handler of flow in water bodies.

Due to the low cost, the availability of related resources (including component model expertise in the Earth and Atmospheric Sciences Department) and its ability to efficiently simulate multiple physical processes in a large region, this study uses the publicly available SWAT-MODFLOW code developed by Bailey et al. (2016) using FORTRAN. Further rationale for using SWAT-MODFLOW lies in the physical processes that are simulated by each component model. Due to MODFLOW's limited strength at simulating unsaturated GW flow and SW processes, SWAT-MODFLOW was chosen over GSFLOW because MODFLOW covers the flow processes associated with rivers and lakes in the latter. If the component models have not been developed beforehand, as in this study, the code used allows for the SWAT and MODFLOW models to be built separately, and in any desired Graphical User Interface (GUI).

Once each model is complete, input files can be created from them. With these, the coupled model runs using a single executable file (Bailey et al., 2016).

#### **1.4. Case Study: Fox Creek, Alberta**

Since the rise in economic potential of hydraulic stimulation in combination with horizontal drilling, the region of Fox Creek, Alberta, has become a key area for the province's oil and gas development (Chevron Canada, 2017). For many operators in the area, the Duvernay Formation is targeted for its unconventional resources, with wells using up to a total of 30,000 m<sup>3</sup> of water to effectively fracture the reservoir (PRCL, 2014), although this value can increase further when targeting formations elsewhere (Johnson and Johnson, 2012). Historically, much of the fresh water required for operations was sourced from the rivers and streams in the region (CSUG, 2016), which resulted in the voicing of considerable concerns from the community about low river flow in the area. Concerns like this contributed to the imposition of stricter industrial extraction regulations in 2015 (AER Bulletin 2015-25). Though extraction of GW from freshwater (or near-fresh) aquifers had occurred before these regulations, there has since been an increase of interest in the use of these resources for their use in hydraulic fracturing operations (Hughes et al., 2017). However, a lack of understanding of the total ground and surface water availability, reliability and their interactions; and limited available projections under future climate change scenarios may restrict future increases in production of energy resources in the region. Therefore, it is important to integrate both SW and GW supply-demand processes in the region to systematically study the future opportunities and conflicts for the industry. This study tests the coupled GW-SW model, SWAT-MODFLOW, by taking the Fox Creek area as a case study to evaluate its ability to simulate a hydro(geo)logically complex catchment. Due to

similarly increasing water use trends in other semi-arid basins with strongly defined seasons such as North Dakota (Scanlon et al., 2016), the findings and workflows of this study can be applied to evaluate GW-SW interaction in nearly any watershed worldwide, particularly when considering the existing range of basins already studied (explained further in Section 1.5) (Sophocleous et al., 1999; Kim et al., 2008; Guzman et al., 2015; Bailey et al., 2016).

## 1.5. Component Model Overviews and Previous Work

### 1.5.1. SWAT: Overview

The Soil and Water Assessment Tool (SWAT) is a physical process-based hydrological model developed by the US Department of Agriculture (Arnold et al., 1998). Developed with the intention of simulating the impacts of land use and climate changes on water quantity, water quality, and food production, SWAT incorporates many different processes such as overland and channel flow, precipitation and temperature (Figure 3), with an emphasis on the accurate representation of surface processes in the top 0-2 m of the soil layer (Neitsch et al., 2009; Bailey et al., 2016). Model calculations for water balance and other physical balances are performed for each HRU, which are defined based on soil, land use and slope data within a subbasin. The water balance equation that is solved for each HRU is as follows (Neitsch et al., 2009):

$$SW_t = SW_0 + \sum_{i=1}^t (R_{day} - Q_{surf} - E_a - w_{seep} - Q_{gw})$$

In the equation above,  $SW_t$  represents the final soil water content,  $SW_0$  represents the initial soil water content on a given day ( $i$ ),  $t$  is the time in days,  $R_{day}$  represents the amount of precipitation on the same day ( $i$ ),  $Q_{surf}$  represents surface runoff,  $E_a$  represents

evapotranspiration,  $w_{seep}$  accounts for water entering the vadose zone, and  $Q_{gw}$  represents return flow. In this water balance equation, each parameter is measured in mm H<sub>2</sub>O and each parenthesized parameter is measured for the given day ( $i$ ). Data from the HRU calculations are then scaled up to provide outputs for river discharge, GW recharge, precipitation patterns, evapotranspiration, and many more factors for each subbasin outlet, making SWAT particularly computationally efficient for long simulation periods (Arnold et al., 1998; Bailey et al., 2016). Based on this definition method, multiple HRUs can be present within a single subbasin, and single HRUs may be present in more than one subbasin. For facilitated visualization of the input and output data, SWAT is linked with ArcGIS, and its data can be viewed as layers within this interface.

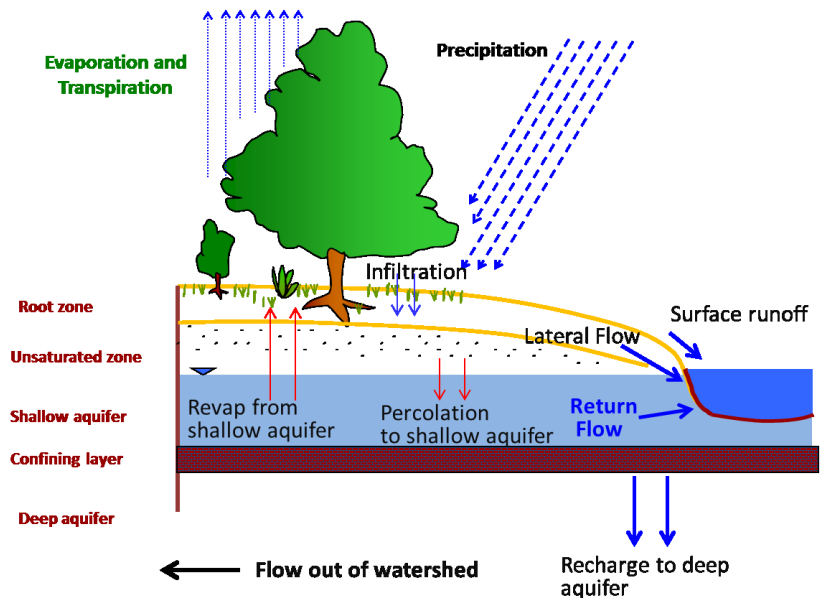


Figure 3: Schematic of the hydrological cycle as represented by the SWAT model (modified from Neitsch et al., 2009).

A notable limitation of the SWAT model is its inability to explicitly simulate dynamic GW flow. Instead, it implicitly represents the effects of ground water by some physical parameters only at

the subbasin level. As such, temporal variation of SW and GW interaction within each subbasin and the GW flow between subbasins is lacking in the model. Due to performing its calculations by individual HRU, the output generated by SWAT's GW module is only available at outlets for each subbasin, yielding a simplistic discharge/recharge result for what could be a very large area.

### 1.5.2. MODFLOW: Overview

Originally developed by the USGS (McDonald and Harbaugh, 1983), MODFLOW is a numerical, three-dimensional groundwater flow model that uses the Finite-Difference equation (based on Darcy's Law and the conservation of fluid mass equation, described below) to simulate saturated flow. Additional processes such as contaminant transport can also be represented through built-in engines (MT3D and RT3D). As a grid-based model, its calculations are performed at nodes located at the centre of each grid cell (Figure 4).

In MODFLOW, GW flow is governed as follows:

Conservation of Fluid Mass:  $-\frac{\partial v_x}{\partial x} - \frac{\partial v_y}{\partial y} - \frac{\partial v_z}{\partial z} = S_s \frac{\partial h}{\partial t}$ , where  $v$  represents velocity,  $h$  represents hydraulic head,  $t$  represents time, and  $S$  is specific storage of the porous media.

Darcy's Law:  $v_x = -K_x \frac{\partial h}{\partial x}$ , where  $K$  is the hydraulic conductivity of the porous media.

Combined GW flow, with infinitesimal differences in the  $x$ ,  $y$  and  $z$ -directions ( $\partial x$ ,  $\partial y$ ,  $\partial z$ ), gives:

$$\frac{\partial}{\partial x} \left( K_{xx} \frac{\partial h}{\partial x} \right) + \frac{\partial}{\partial y} \left( K_{yy} \frac{\partial h}{\partial y} \right) + \frac{\partial}{\partial z} \left( K_{zz} \frac{\partial h}{\partial z} \right) + W = S_s \frac{\partial h}{\partial t}$$

In the above equation,  $K$  replaces the  $v$  terms, and  $W$  represents outside influences such as pumping wells or sinks. If infinitesimal differences ( $\partial x, \partial y, \partial z$ ) are replaced by finite differences ( $\Delta x, \Delta y, \Delta z$ ), an example equation defining GW flow in the  $x$ -direction is as follows:

$$\frac{\partial}{\partial x} \left( K_{xx} \frac{\partial h}{\partial x} \right) = \frac{1}{\Delta x} \left( K_{i+1/2} \frac{(h_{i+1} - h_i)}{\Delta x_{i+1/2}} - K_{i-1/2} \frac{(h_i - h_{i-1})}{\Delta x_{i-1/2}} \right)$$

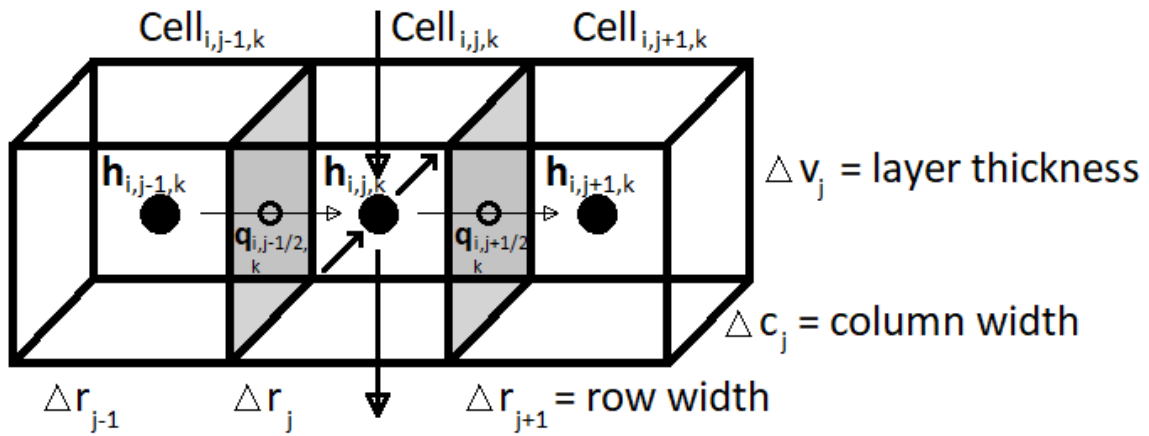


**Figure 4: A diagram of box-centered flow, representative of how MODFLOW performs calculations. The Finite-Difference equation is evaluated at nodes located in the center of each cell, in three dimensions, determining flux in and out.**

Although it is, at its heart, a FORTRAN computer code, MODFLOW is available to be used in Graphical User Interfaces (GUIs) such as Visual MODFLOW (Waterloo Hydrogeologic, 1994), which will be used in this study. Building models using this interface allows scientists without backgrounds in coding to translate their conceptual models to numerical simulations in a user-friendly way.

The engines used for numerical simulations in MODFLOW have gradually improved over time. This study uses MODFLOW-NWT (Newtonian Solver) (Niswonger et al., 2011), which allows for the repeated drying and re-wetting of grid cells over the simulation period. As the study area is subject to wide seasonal climate fluctuations, the MODFLOW-NWT engine allows for a more faithful representation of the changing hydraulic heads found in Alberta.

Similar to SWAT, MODFLOW is not without its limitations. Its grid-based method of flow calculation can be both a boon and a hindrance, with a constant trade-off taking place between fine grid discretization and computational time. In addition, it takes its boundary conditions from surface processes, so these could be limited and uninformed in areas with little available data. MODFLOW is also unable to incorporate many surface processes such as wind, temperature fluctuation and soil/land use changes into its simulation engines, being largely limited to precipitation inputs and either constant heads (and water bodies, which act as semi-constant heads) or head-dependent flux boundaries to represent what occurs at the surface.

### *1.5.3. Previous Work*

#### Work in the Study Area

In the province of Alberta, there have been multiple projects implemented to separately characterize SW and GW flow. Of particular interest to this project, the Alberta Geological Survey (AGS) has an ongoing objective of providing detailed GW information on the Fox Creek region (Smerdon et al., 2016), as well as other areas of interest in the province. This is to be accomplished by developing a three-dimensional GW flow model that conforms to the regional hydrostratigraphy of the study area, and will include rock units of Quaternary, Neogene and

Upper Cretaceous age. Elevations of these units were obtained through various methods that included legacy boreholes, water wells, gamma logs and field mapping (Smerdon et al., 2016). An eventual goal of this work was to assess the interaction of GW and SW in the region, which led to the collaborative effort with the AGS that, in part, led to the research described here. The bedrock elevation data used by the AGS was included in this study, and covered the study area's southern portion.

With regards to work on modelling SW in the study area, Faramarzi et al. (2015, 2017) completed a comprehensive Alberta-wide SWAT model. This model has been thoroughly calibrated and validated using the monthly streamflow data of 130 hydrometric stations for the 1980-2010 period. River and stream discharges were compared to Environment Canada's records for the 1983-2007 period (with a three-year warm-up period, also used for this study's SWAT model) (Faramarzi et al., 2015). This regional model helped to identify key areas, or hot spots, in the province where more work was needed (including the Fox Creek region). In addition, the upstream portions of each major river basin were subject to higher model uncertainty, with the lack of local stream gauges and the implicit nature of the SWAT model's GW outputs contributing as potential reasons for that uncertainty (Faramarzi et al., 2015). The lessons learned through this large-scale modeling exercise (including a need for more detailed GW-SW interaction information) were used to develop a refined SW component model for this coupled study.

#### Integrated SWAT-MODFLOW Models

Though the coupling of SWAT and MODFLOW to make an integrated GW-SW model has been successfully applied to various basins throughout the world (Sophocleous et al., 1999; Kim et al., 2008; Guzman et al., 2015; Bailey et al., 2016; Bailey et al., 2017), SWAT-MODFLOW is still a relatively novel technique, and has not seen widespread use outside of academia, nor in regions with pronounced winter seasons such as Canada. This section outlines the coupled models that have been implemented thus far.

### Rattlesnake Creek Basin

At its time of development, SWATMOD, the first successful attempt to integrate a SWAT and a MODFLOW model by Sophocleous et al. (1999), was unprecedented. Applied to the Rattlesnake Creek Basin of Kansas, SWATMOD is a basin-wide model that was specifically built to simulate low-flow, or drought, conditions. SWAT and MODFLOW were chosen as component models in order to represent the greatest number of physical processes in the area, as a primary goal of this work was to provide a tool that could be used for long-term forecasting (Sophocleous et al., 1999). In order to successfully link the two models, both had to be modified. When SWATMOD is run, each model calls a subroutine program: HYDBAL for SWAT, and MODSWB for MODFLOW. HYDBAL passes data between SWAT and MODFLOW for each time step, and it allows the coupled program to provide hydrologic balance outputs. MODSWB acts as a method of connecting SWAT's subbasins with MODFLOW's grid cell network.

As the earliest example of a coupled SWAT-MODFLOW model, the study completed by Sophocleous et al. (1999) was not without its limitations. As the computational burden would have been too great if the MODFLOW model was run on a daily time step, it was instead run with monthly steps, while SWAT ran with daily steps. However, due to the study being intended for long-term (decadal) use, this limitation was considered to be fairly minor. Overall, the study

performed by Sophocleous et al. (1999) laid the groundwork for all subsequent studies that coupled SWAT and MODFLOW models.

#### Musimcheon Basin

Built as a way to overcome the shortcomings of SWAT's limited GW calculation ability, Kim et al. (2004a, b) first developed a coupled GW-SW model in 2004. To accomplish this, an HRU-cell conversion interface was developed using GIS data. This allowed SWAT to use MODFLOW as a GW subroutine instead of its existing GW programming.

The methodologies developed in these studies were applied to the Musimcheon Basin of South Korea (Kim et al., 2008), which has an area of 198 km<sup>2</sup>, and was divided into 34 sub-basins by SWAT. The MODFLOW component used a grid size of 100 x 100 to better match the SWAT model's HRUs with MODFLOW's grids. This resulted in 223 rows and 214 columns in the model, with three layers that represent the area's aquifers. The model's GW limits matched those of the SW basin, to focus on the relatively local flow within the basin. When calibrating the GW component, the most sensitive parameters were hydraulic conductivity and storativity. This process was carried out primarily by trial and error by iteratively adjusting these parameters.

This study was the first SWAT-MODFLOW application to include water wells in the basin with active pumping schedules. With the majority of wells located in the downstream portion of the study area, drawdown was tracked for the simulation period. Due to the wells' pumping rates reflecting real-world conditions, they contributed to the improved calibration of the SWAT-MODFLOW model. Although this historical pumping data was useful for the field representation, it was difficult to forecast impacts due to continued pumping, as it was out of the scope of the study (Kim et al., 2008).

## Fort Cobb Reservoir Experimental Watershed

Located in a region of high agricultural activity, the objective of the study performed by Guzman et al. (2015) was primarily to monitor and forecast the impacts of anthropogenic activity on a man-made watershed. To do so, a SWAT-MODFLOW code, named “SWATmf,” was developed using Guzman’s SPELLmap software (Guzman et al., 2013). SPELLmap itself was developed two years prior, and acts as a unified framework for analyzing surface hydrology. Using this software, one is able to prepare, analyze and model large sets of environmental data, and so adding GW-SW interaction into this framework was a logical next step.

The project’s MODFLOW model was built using “SWATmf-app,” which acted as the study’s SWAT-MODFLOW project manager. SWATmf-app also allows for the visualization and editing of SWAT within the same interface, thus allowing the models to be built in tandem. Intended as a multi-purpose resource, the Fort Cobb Reservoir Experimental Watershed (FCREW) was artificially built above the Rush Spring aquifer in Oklahoma, USA, and covers 780 km<sup>2</sup>. Multiple HRUs were defined within each subbasin, for a total of 1001. The study’s corresponding MODFLOW model was built with a 300 x 300-meter grid, resulting in a 120 x 144 grid for the area. To represent the aquifers, four layers were used, with one primary aquifer and other rock units of variable hydraulic conductivity.

## Sprague River Watershed

The most recent of the SWAT-MODFLOW models and codes developed is reported in the study by Bailey et al. (2016), who modeled the Upper Klamath Basin of Oregon. The Upper Klamath Basin’s Sprague River watershed drains a significantly larger area than the previously discussed Musimcheon Basin and FCREW, at 4,000 km<sup>2</sup>. This project takes two separately calibrated

models (Gannett et al., 2012; Records et al., 2014), and uses MODFLOW as a subroutine of the SWAT code to provide it with more accurate GW outputs. Though many tributaries exist in the region, the Sprague River is dominant, and was thus the principal river included in this project's MODFLOW model.

The SWAT component of this model was built from four separate SWAT-model components, each covering different river systems. Together, these parts have an area of roughly 4,100 km<sup>2</sup>, and used a 30-meter resolution DEM as a source for its surface topography data. The model's HRUs were created to correspond with the area's separate agricultural fields, and these HRUs are how SWAT communicates with the grid cells of MODFLOW. In addition to the communication between HRUs and grid cells, the HRUs have also been disaggregated (called DHRUs), which enables the HRU calculations to be geo-located.

This MODFLOW model's development forged a new path for integrated tools by using MODFLOW's Newtonian solver algorithm (MODFLOW-NWT), which is significant for its ability to run with grid cells repeatedly drying and re-wetting. This process represents the real physics of unconfined aquifers with considerably more accuracy than previous MODFLOW engines. Spatially, the MODFLOW model has a total area of 20,000 km<sup>2</sup>, and was built with 285 rows and 210 columns, with a grid size of 762 m. Three layers were defined, which correspond to the area's hydrogeologic units. Similar to the model developed by Kim et al. (2008), MODFLOW acts as a subroutine within SWAT, replacing the groundwater processes to provide outputs based on the Finite-Difference equation of groundwater flow. The coupled SWAT-MODFLOW tool was run for a time period of 34 years (1970 – 2003) with daily time steps. If, as part of the model run, MODFLOW is set to have time steps of greater than one day, the code imposes a daily time step instead.

## Little River Experimental Watershed

The primary purpose of this recent study by Bailey et al. (2017a) was to supplement Bailey's previous SWAT-MODFLOW code (Bailey et al., 2016) by showcasing SWATMOD-Prep, a new Graphical User Interface (GUI) that facilitates the coupling of SWAT and MODFLOW. This new GUI allows an existing SWAT model to be coupled with a new MODFLOW model that is built within the GUI itself. SWATMOD-Prep is a significant step in making GW-SW interaction software more accessible. It can currently only couple a SWAT model with a one-layer MODFLOW model, but future developments may be able to incorporate more complex GW models.

The Little River Experimental Watershed of Georgia, USA, covers an area of 334 km<sup>2</sup>, with surface elevation and hydrology represented by a 30-m resolution DEM (Bailey et al., 2017a). Of note is the SWAT model's fine discretization, with the final model having 240 subbasins and 1308 HRUs. The watershed experiences regular rainfall events that are short, but high in intensity. Like the previous model built by Bailey et al. (2016), this study uses the Newtonian Solver (MODFLOW-NWT) as MODFLOW's engine. Compared with the complexity of the SWAT component, the MODFLOW model is relatively simple.

A key learning from this study was that higher computational efficiency is observed when the MODFLOW grid cells are a multiple of the raster grid size used for SWAT's HRU and subbasin definition. If this is the case, then the two models can communicate more effectively.

Historically, SWAT-MODFLOW models have had run times that last multiple hours to days, yet this interface can run a coupled model in 15 seconds. This is, however, taking the fact that the MODFLOW model has only one layer into account, and the run time will inevitably increase with the complexity of the models.

A summary table of the major developments in SWAT-MODFLOW tools, as well as brief descriptions of HGS and GSFLOW, has been included in the Appendix (Table A1).

## **1.6. Objectives and Hypotheses**

### *1.6.1. Gaps in Knowledge*

Thus far, successfully implemented SWAT-MODFLOW models have covered regions with more temperate climates. As such, creating a representative model for an area such as western Alberta is accompanied by additional challenges, particularly with respect to data requirements. For example, the latitude of the study area and its proximity to the Rocky Mountains necessitates the addition of snowfall data, which varies throughout the simulation period. Each of the new inputs influence the model, and that influence is especially heavy in the case of snowfall data. As a result of snow accumulation on the ground surface, as well as freezing of rivers in the area, SW discharge and GW recharge are significantly lower in winter months than in summer months, with the most pronounced recharge observed in the months of April to June.

With respect to the GW component of the model, the maximum number of MODFLOW layers in a documented SWAT-MODFLOW model has been four so far (Kim et al., 2008; Guzman et al., 2015; Bailey et al., 2016), with a focus on more local flow patterns for each study area. The model built in this study will be the first to include a GW component that primarily focuses on the area's bedrock geology, as the study area houses a complex subsurface with many pinching-out and outcropping formations (discussed further in Section 2.2). In addition, the SWAT-MODFLOW model developed in this study covers a larger area than any applied before, which accounts in part for the wide variation in climate, surface elevation and hydro(geo)logy.

In addition to the above, implementing a SWAT-MODFLOW model with the intention of gaining more knowledge on the potential magnitudes of natural and human influences on a study area has not been done to this extent. Although previous studies have considered human influences on basins (Kim et al., 2008; Guzman et al., 2015), this will be the first to incorporate a combination of well pumping and climate change, allowing the two to be compared over the simulated periods. This study aims to address the above gaps in knowledge by posing the following question: how can we use SWAT-MODFLOW to assess the relative influences of new and combined scenarios on a complex watershed?

### *1.6.2. Study Goals*

Due to the novelty of SWAT-MODFLOW as a GW-SW modelling tool, the extent of its use has been largely limited to those who developed SWAT-MODFLOW codes (Sophocleous et al., 1999; Kim et al., 2008; Guzman et al., 2015; Bailey et al., 2016). Furthermore, the models developed in each of these studies covered smaller study areas, with less complex hydrogeology and were mainly intended for understanding local water changes. Prior to this study, Bailey's Sprague River Watershed model (2016) was the largest at roughly 4,100 km<sup>2</sup>. Other models range in size to fit various goals, with some as small as 198 km<sup>2</sup> (Kim et al., 2008), and most having study areas in the high hundreds to low thousands of square kilometers (Guzman et al., 2015). In addition, the successfully implemented SWAT-MODFLOW models thus far have had less complex hydrology and hydrogeology, with each of the MODFLOW components having a maximum of four layers, thus focusing on more local GW flow patterns (Kim et al., 2008; Guzman et al., 2015). By virtue of being in western Alberta, the case study area (the Little Smoky River watershed) is subjected to highly variable, yet predictable, climate patterns. Like most Canadian watersheds, the Little Smoky River experiences relatively high discharge during

spring and summer months, with next to no flow during the winter months. This, in turn, affects the hydrology of the area's basins. With the Little Smoky River's headwaters located at elevations of more than 1200 meters above sea level, snowfall is an influence that must be considered for the most realistic representation of the area's climate. In addition, the Western Canadian Sedimentary Basin is a region of high geological variability. Many of the formations found at great depth in the Rocky Mountains outcrop to the northeast. Due to the differing lithologies and elevations of these units, those with aquifer potential have a complex hydrogeology, made even more so by their heterogeneity in terms of their hydraulic conductivity and storage properties (Farvolden, 1961; Hughes et al., 2017). Further to these hydrologic and hydrogeologic conditions, the importance of this study's chosen watershed in water supply and demand challenges, i.e., conflicts between energy production, food production, and environment, makes it an ideal case study to test the SWAT-MODFLOW model under a climate change projection for studying the water-food-energy nexus. This was taken a step further by applying a high-rate pumping simulation to the climate change forecast to evaluate the significance of natural and anthropogenic influences on the study area. **The primary objective of this study was, therefore, to test SWAT-MODFLOW's ability to simulate a large region with heterogeneous natural features and diverse anthropogenic factors, and considering more complex climate and water use scenarios, with a greater focus on bedrock hydrogeology than in earlier studies.** This was done to achieve the goal of further understanding the natural and anthropogenic influences that play a part in the WEF nexus for management and planning.

### *1.6.3. Hypotheses*

Due to the number of new stressors and factors that are being introduced in this study, it is likely that the integrated SWAT-MODFLOW model will encounter numerous errors before being able

to run effectively. Each additional stressor and parameter that is included in the model also introduces a level of uncertainty about results. Though based on field data and literature, the calibration of such a model will be subject to non-uniqueness, with many possible parameter value combinations producing an adequate model (explained further in Section 2.3).

As determined by Bailey et al. (2016), even a coupled model with three MODFLOW layers takes more than ten hours to run. This means that if this study's model runs for the entire simulation period of 9131 days, the computational time will likely be in excess of 12 hours. In the process of building such a model, run time is always a consideration. The ability to repeatedly run a model is valuable for both calibration and for adding new stressors (such as pumping wells) to the system. Since running a coupled SWAT-MODFLOW model takes more time than running either component model by itself (Bailey et al., 2016), it is ideal to minimize run times in the SWAT and MODFLOW models before coupling, thus allowing the integrated tool to be run more often during the calibration/validation process. While acknowledging that fine resolution is indeed important for an accurate hydrological model, this study must account for the additional influences of snow outputs, highly variable discharge, and a seven-layer MODFLOW model, which will likely increase coupled run times and make a fine spatial discretization of cells in the model implausible. Although both component models were built as part of this study, the representation of the conceptual model within each interface differs slightly based on their numerical computation methods (grid-based vs. HRU-based), and coupling may therefore take multiple attempts.

With respect to the coupled model's ability to simulate the study's watershed, we predict a similar level of competency to each of the component models after calibration, as the SWAT-MODFLOW model's performance depends on accurate components. What will set the coupled

model apart from its components is its ability to display GW-SW exchange values for each MODFLOW river grid cell, which are expected to vary considerably, based on their location and the simulation month. The effects of climate change on the forecast scenarios are expected to be minimal in comparison to those of the pumping scenarios, as the simulation years only cover up to 2034 (discussed further in Section 2.4). Therefore, we hypothesize that direct anthropogenic activity will have more immediate effects on the watershed than climate change.

## 2. METHODS

### 2.1. Study Area

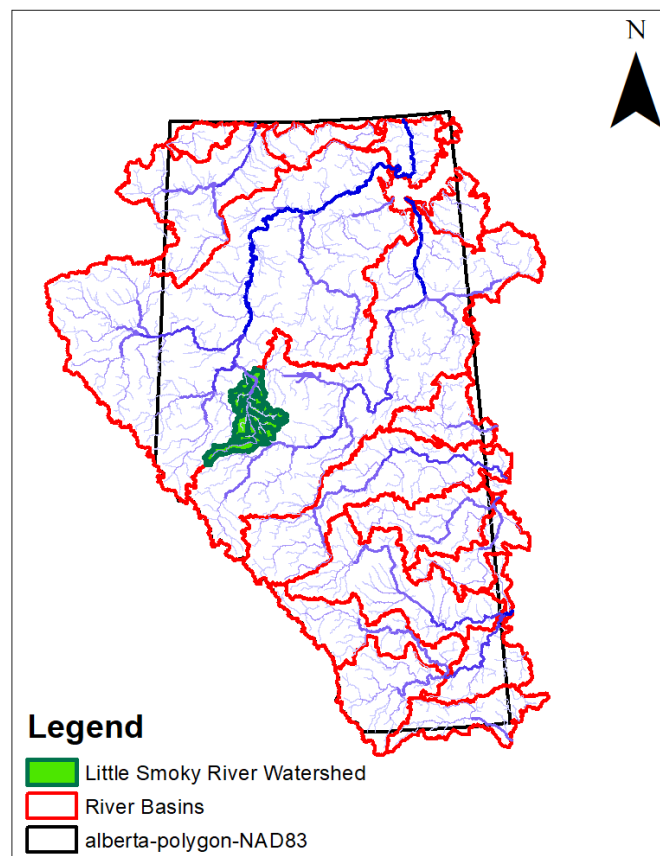


**Figure 5: The study area (Little Smoky River Watershed), shown within the province of Alberta, Canada.**

The Little Smoky watershed of Alberta (Figure 5, above) covers 11,494.22 km<sup>2</sup> of land, with diverse landscapes found within. Much of the area's southwestern reaches are subalpine, with elevations ranging from 1000-1400 meters above sea level. This area provides essential habitats to a plethora of flora and fauna, some of which are ecologically significant and protected. The presence of multiple caribou populations in the area prohibits the development of infrastructure such as pipelines through their range. Other significant fauna found within the Little Smoky area include grizzly and black bears, mountain goats and moose, while the Little Smoky River itself houses a vital population of Arctic grayling. This river is considered a "blue ribbon native fishery" (Campbell, 2015).

The existence of such a rich ecosystem imposes demands for water on top of those placed by industries such as agriculture and energy. In addition to effects on the area's human populations, the watershed's flora and fauna may be impacted when freshwater is extracted for industrial purposes. Similar demands on water resources occur in numerous watersheds worldwide that are subject to energy and agricultural development. Therefore, building a model that can determine changes to both GW and SW is essential to understanding how water in the study area can be exploited sustainably.

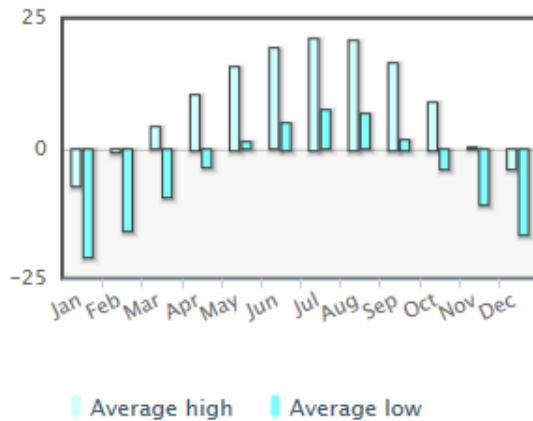
### *2.1.1. Surface Hydrology*

As is the case with many of Alberta's rivers, the Little Smoky River's headwaters are found within the foothills of the Rocky Mountains. Acting as a tributary to the Peace River, the Little Smoky River's waters eventually flow into the Mackenzie River and the Arctic Ocean.

The hydrology of the Little Smoky area is heavily influenced by the seasons. As the Little Smoky River is fed by the mountains, more discharge is recorded in the spring and summer months, which is the result of the yearly spring snowmelt and increased precipitation. Similarly, a pronounced decrease in discharge is consistently recorded in the autumn and winter months, coinciding with lower precipitation levels and freezing. Like much of Alberta, the area is subjected to periodic droughts and floods (Alberta Water Portal, 2017), which can heavily influence the industries there, as well as locally-changing hydrologic flow patterns. The downstream portion of the Little Smoky River watershed levels out into forest and prairie land, much of which is dominated by agricultural and upstream oil and gas activity, with the forestry industry also having a presence.

The combination of hydrological inputs into this area form a complex surface water system, with rain, snowfall and runoff all playing roles. The Little Smoky River's location in west-central Alberta means that it experiences a generally semi-arid climate. However, although the annual means for temperature and precipitation are roughly 2.5 °C and 515 mm, this climate is highly variable in terms of both its temperature and precipitation, even on a monthly basis, as seen in Figure 6. Due to the larger study area than previous studies, the Little Smoky River watershed also incorporates a wider range of elevations (from foothills to prairies), which brings with it more soil and land use types. As such, the area makes for a complex basin to apply a coupled GW-SW model.

### Overview: Temperature (°C)



### Overview: Precipitation

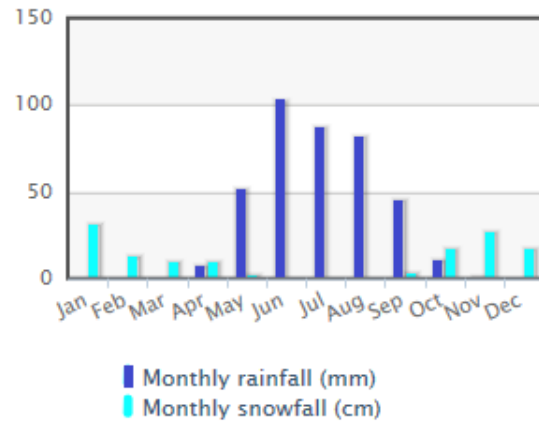


**Figure 6: Average temperature and precipitation graphs, taken at the Fox Creek Junction Station, Alberta (modified from The Weather Network, 2018).**

### Climate change

Of increasing concern in the study area are the effects of climate change on the region's flora and fauna, as well as the hydrological system. The most significant recent change in Alberta, already subjected to a range of weather, is the widened variability in possible climatic conditions (Alberta Water Portal Society, 2017). Within the last twenty years, Alberta has already had two major floods, signifying a possible increase in the amount of extreme weather that will be experienced going forward, including events on the other end of the spectrum such as droughts. Global temperatures are consistently exceeding the historical averages, cementing the fact that anthropogenic activity is a heavy contributor to climate change (IPCC, 2014). As we begin to understand the types of climate that Alberta will experience, it is becoming increasingly important to develop models and databases to determine the effects of these changes on water resources, so that our infrastructure and food supplies may be able to tolerate more extreme conditions. Of course, climate change is being experienced the world over, and so the learnings

taken from this study (and the climate change models used, further discussed in Section 2.6) can be applied to other basins.

### 2.1.2. Geology and Hydrogeology

Given the size of the study area, the depths and properties of the underlying rock formations vary considerably. In this project’s study area, similar to the rest of Alberta’s Rocky Mountains, various formations outcrop or come close to outcropping, with a general trend toward the northeast (Wright, 1984; also see Figure 10). Quaternary sediments cover the majority of the study area’s southern near-surface, with various members of the Paskapoo Formation directly underlying. However, in the downstream (northern) area of the Fox Creek watershed, older formations begin to outcrop, such as the Scollard, Battle and Wapiti/Belly River Formations (see Figures 7 and 10).

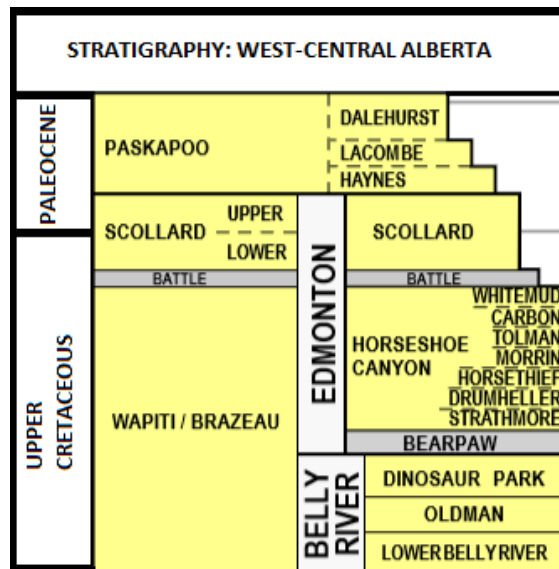


Figure 7: Representative stratigraphic column for West-Central Alberta (modified from AGS, 2015).

Many rock units throughout Alberta have been evaluated for aquifer potential, including the Basal and Upper Belly River, the Edmonton-Upper Wapiti, and the Scollard Formations (Bachu

and Michael, 2002). Of the subsurface aquifers specifically used for hydraulic fracturing-related activities, however, the Paskapoo Formation is the principal unit of interest. Reasons for this include its location beneath areas of industry activity, its proximity to the surface, and its formation water, which have low total dissolved solids (Hughes et al., 2017). A particular point of interest in this study is this formation's interaction with SW. As a shallow unit, the spatial and temporal scales at which water interaction and movement occur are much more local than they are for deeper aquifers. This allows for variable exchanges of SW and GW, within the study area and within a timeline of human significance (Tóth, 1963).

#### Wapiti, Bearpaw, Whitemud-Battle, Scollard Formations

Deposited in the Campanian and Maastrichtian stages near the end of the Cretaceous Period, the Wapiti Fm. is a clastic wedge comprised primarily of fluvial sandstone and siltstone (Fanti and Catuneanu, 2009). Overlying the Lea Park and Puskwaskau Formations, there is a conformable transition between marine shales and non-marine fluvial deposits observed in the Smoky area of Alberta. In the southern portion of the study area (and continuing further to the south), this formation is equivalent to multiple formations, including the Belly River, Bearpaw, Horseshoe Canyon, Whitemud and Battle Formations (Dawson et al., 1994).

The Wapiti Fm. varies widely in thickness, generally growing thicker in a southwest trend toward the Rocky Mountains. At its deepest in the study area, the Wapiti is roughly 1300 meters thick, thinning to 300 meters in the northeastern portion of the Little Smoky River area (Smerdon et al., 2016). The stratigraphic top of this formation also displays significant variance in depth, appearing at roughly 275 meters above sea level near the mountains (surface elevation in this area is ~1200-1400 meters), and shallowing toward the northeast to become the shallowest bedrock layer in the northern portion of the study area (Smerdon et al., 2016).

Only appearing in the southernmost reaches of the study area, the Bearpaw Fm. is principally a marine deposit, with the majority of the succession consisting of laminated shale. Other lithologies present include siltstone and claystone, as well as infrequent sandstone beds (Dawson et al., 1994).

The Whitemud-Battle succession appears as the thinnest layer in the study area, and thus the thinnest in the representative MODFLOW model. With each of these formations being very laterally continuous (Dawson et al., 1994), they overlie the Wapiti Fm. in the majority of the study area.

Though dominated by sandstone and siltstone, the two-member Scollard formation is better known for the economically significant coal seams that it houses in its upper member (Dawson et al., 1994). Similar to other formations in the study area, the Scollard thickens toward the foothills (Dawson et al., 1994), and ranges from 0 to over 200 meters thick in the study area (Smerdon et al., 2016).

#### Paskapoo Formation

Deposited in the Paleogene, the Paskapoo Fm. is a highly heterogeneous fluvial deposit (Hughes et al., 2017) that appears as the shallowest bedrock layer in most of the Little Smoky River area. Even within the study area, this formation exhibits a high range in thickness, following a thickening trend toward the foothills (Dawson et al., 1994; Smerdon et al., 2016).

Three primary units, or members, within the formation have been identified in the study area based on lithological differences. From oldest to youngest, they are the Haynes aquifer, the Lacombe aquitard, and the Sunchild aquifer (Hughes et al., 2017; Lyster and Andriashek, 2012). Equivalent members exist elsewhere in the province under different names, such as the Dalehurst

member, which is an alternative unit to the Sunchild (Demchuk and Hills, 1991; Lyster and Andriashek, 2012). The porosity and hydraulic conductivity observed by Hughes et al. (2017) in these members share a linear relationship, with higher values for both porosity and hydraulic conductivity recorded in the Haynes and Sunchild aquifers. In the study completed by Hughes et al. (2017), average conductivities were  $1.3 \times 10^{-6}$  m/s and  $4.4 \times 10^{-9}$  m/s for the sandstone and mudstone/shale units respectively, primarily obtained via air permeameter testing.

Known for its aquifer potential (Hughes et al., 2017), this shallow formation is an important, near-fresh source of water for many Albertans, and plays host to a multitude of water wells throughout the province (Grasby et al., 2008). Although the bulk of these wells are located within the southern part of the province, upstream producers have begun to exploit this formation (among others) to use its water for their hydraulic stimulation operations. As explained above, the shallow nature of this formation allows for pronounced interaction between its GW and the surface water system, and its many legacy wells (as well as some monitoring wells) help to capture snapshots of this interaction in the study area.

## **2.2. Model Development and Input Data**

### *2.2.1. SWAT Model Development*

ArcSWAT 2012 was used to build the study's SWAT model due to its ability to be visualized in ArcMap. A Digital Elevation Map (DEM) was then imported, and used to delineate the watershed into 28 subbasins (Figures 8A and 8B) and to replicate the area's water network (primarily the Little Smoky River). The model calculates the area's direction and accumulation

of surface water flow based on low points in elevation and represents, in each subbasin, a tributary stream that eventually joins into the Little Smoky River. Upon defining the watershed's main outlet (or outlets), the boundaries and hydrologic parameters of the entire basin are then delineated. For this study's SWAT model, the entire watershed's primary outlet is located at the area's northernmost point, in Subbasin 1 (of 28).

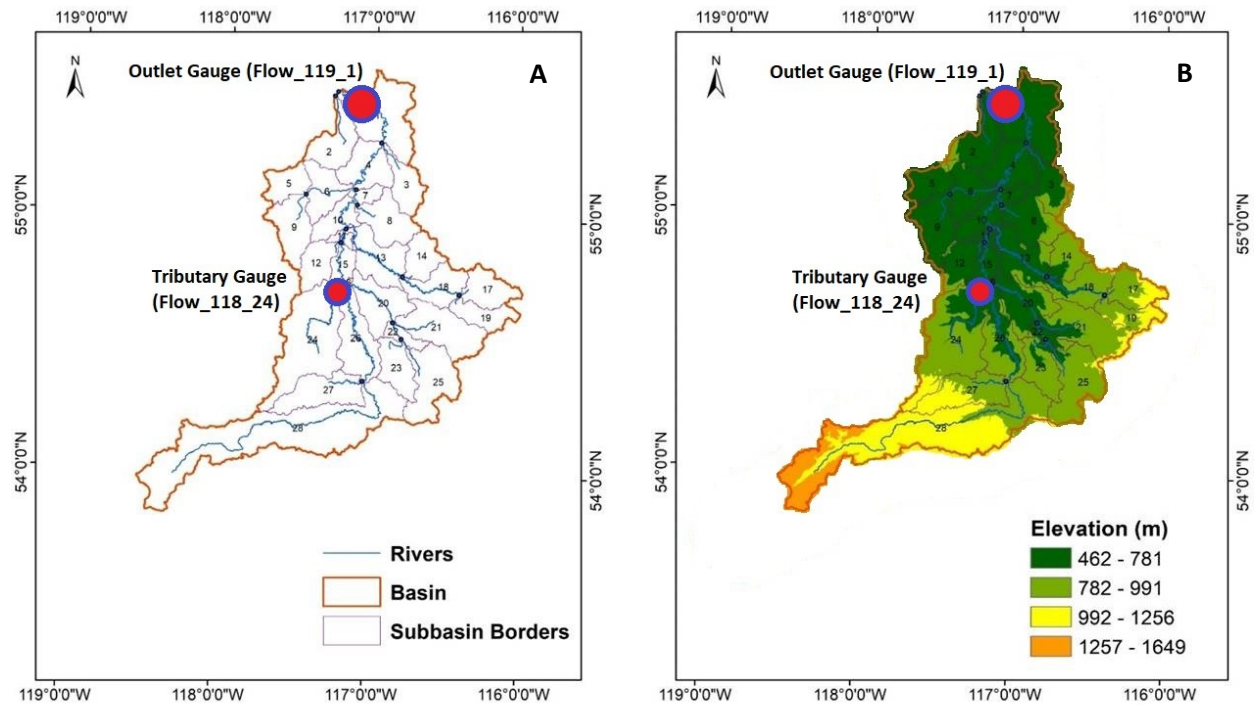


**Figure 8: (A) shows the Little Smoky River watershed (outlined in orange), displaying the study's delineated subbasins, and (B) displays the area's varying elevation. The basin's primary outlet is in subbasin 1, located at the northernmost point of the SWAT model.**

Similar to applying a DEM to the study area, digital maps for both soil and land use were available to use for the Little Smoky River Watershed (Government of Canada, 2015, 2017). As seen in Figures 9A and 9B, respectively, 20 types of soil and 13 land use types exist in the area. The study area's various land use types correspond loosely with the elevations at which they are

found. Southern subbasins are dominated by evergreen forests (FOER land use type, light blue), and correspond with areas that are subalpine to alpine. Agricultural activity (AGRR, brown) is more pronounced as ground elevations level out in the northern portion of the watershed. Throughout the Little Smoky River watershed, deciduous forests (FRSD, dark blue) can be found as well, although these are also more prominent in the area's northern subbasins. Similar to the correlation between land use and elevation, the relation between soils and elevation can be observed fairly clearly. Many of the dominant soil types observed in Figure 8A correspond roughly with the land use types in Figure 8B, although each area's dominant land use type may have more than one soil type associated with it.

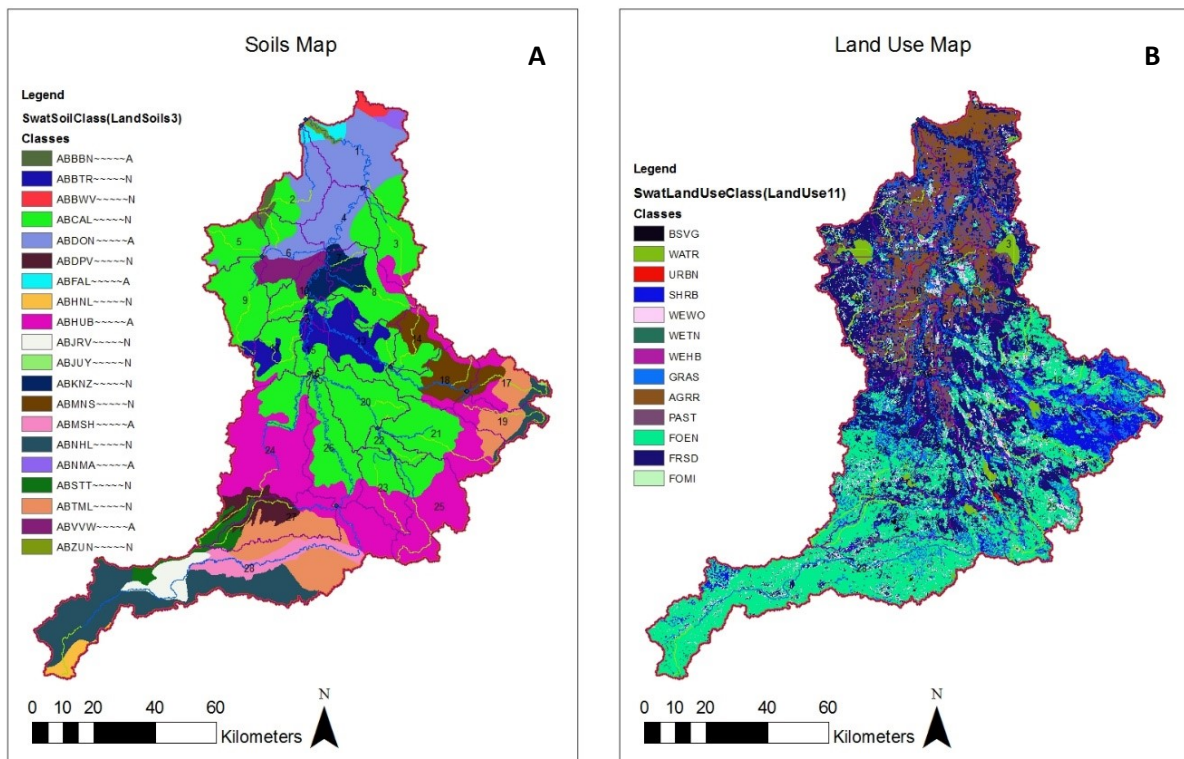


**Figure 9: (A) shows the Little Smoky River's soil types, and (B) displays the land use types. The watershed's soil and land use types roughly correspond to the elevations at which they are found.**

After data for soil and land use was included, we chose a multiple-slope model to better represent reality. We opted for three slope classes: 0-5% incline, 5-10% incline, and over 10% incline. With the model's streams, sub-basins, soils, land use and slopes all in place, HRUs could then be delineated. HRUs (Hydrological Response Units) are sub-sections of the model that are generally smaller than sub-basins. This further breaks the spatial units up into pockets with similar properties to represent local soil, land use, slope characteristics (Bailey et al, 2016). Since they are defined by the dominant soil, land use and slope traits of a watershed, HRUs may not comply with the spatial boundaries of subbasins. Instead, SWAT's calculations are performed for each HRU, and then the results are scaled up to represent values at subbasin outlets, thus producing outputs for each subbasin and every time step. To define the HRUs in the Little Smoky River watershed, we chose to do so with land use, soils and slope weighted at 40%, 30% and 30% respectively, resulting in the creation of 40 HRUs for the study area.

This distribution causes the model to be more computationally efficient. However, it assumes that the qualities found in the HRU-defined areas hold true throughout the subbasins in which they are found, and thus some detail may be missed when compared to a model with more HRUs defined. However, with the potential for coupled SWAT-MODFLOW models to have extended run times (Bailey et al., 2016), the above distribution was chosen to minimize coupled run times, and therefore expedite the calibration process. Moreover, the ability to run a model multiple times per day is ideal for multi-scenario analyses, such as climate change simulations (to be discussed further).

The final major step was to incorporate historical weather data in the model. These data included precipitation, temperature, relative humidity, wind speed, and solar radiation, all for the time period of 1983-2007 (25 total run years). Due to the study area having highly variable climate,

snowfall also had to be simulated. However, SWAT requires no snow-related input; instead, it is generated during the model run and produced as an output. A table listing the sources of all model data can be found in the Appendix (Table A2).

### *2.2.2. MODFLOW Model Development*

Construction of the MODFLOW component to this study was done using the Visual MODFLOW Classic Interface, run on a Windows 8.1 operating system. To allow for the drying and re-wetting of grid cells over a transient simulation, the MODFLOW-NWT (Newtonian Solver) engine was used (Niswonger et al., 2011), similar to the models used by Guzman et al. (2015) and Bailey et al. (2016). This facilitates computation in the case of highly variable hydraulic heads in any given area within the model region.

The model area for this component was 44,954.65 km<sup>2</sup>, with a length of 195.455 km in the x-direction and 230 km in the y-direction. Based on the lengthy run times of previous SWAT-MODFLOW models (Bailey et al., 2016), discretization for this model was intentionally kept coarse to ease the computational burden once coupled with SWAT. A 100 x 100 grid was used, with each grid cell having dimensions of 1.95 km x 2.30 km. While this indeed does take away from detail in the x-y directions, the MODFLOW component remains relatively complex compared to those used in previous SWAT-MODFLOW models by virtue of its many layers, and the heterogeneous hydraulic conductivity found within these layers (thus maintaining variability in K in all three dimensions).

Vertically, the MODFLOW model was divided into seven layers, each corresponding to a geological unit. To accurately represent these formations and their dipping trend toward the

Rocky Mountains, elevation data was required. This was primarily provided as part of a collaboration with the Alberta Geological Survey (AGS), who had previously begun work on developing a MODFLOW model for the same region. This elevation data covered this study's area up to  $y = 195$  km, with the remaining area's elevation data coming from well logs in AccuMap®. Although the formation elevations are highly variable, a uniform model bottom of 1250 meters below sea level was included to allow further possible water flow in areas with shallow bedrock formations (the northern end of the model, see Figure 10).

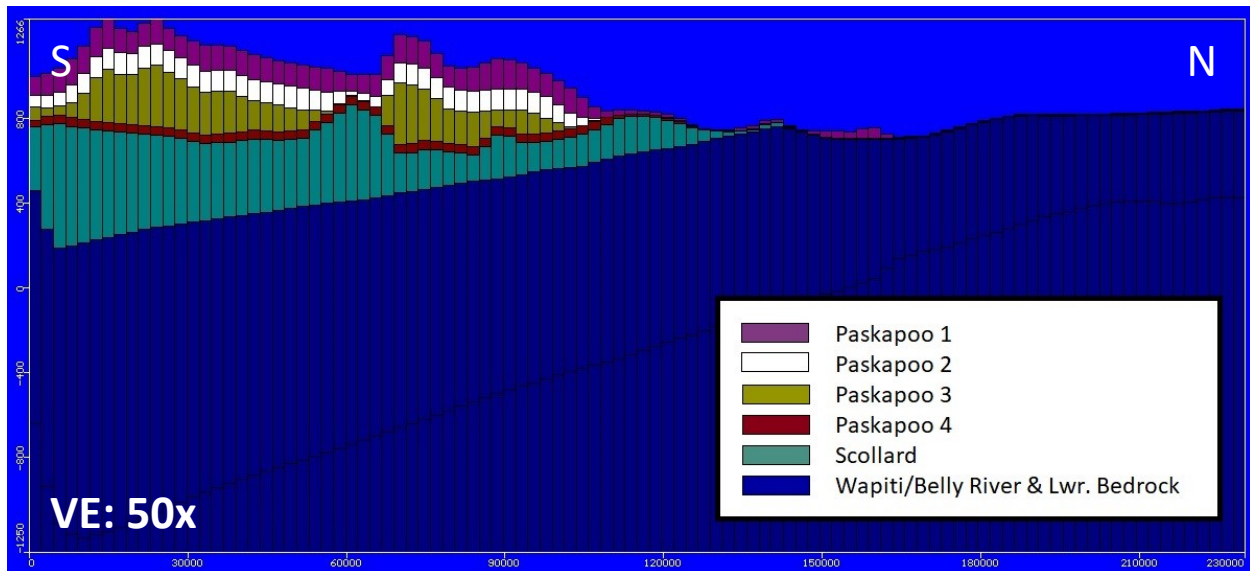


**Figure 10: South-north cross-section of the MODFLOW modelled area, displaying the geological units present (vertical elevations range from 1250 m below sea level to 1250 m above sea level).**

Each rock unit has unique hydraulic conductivity ranges, which are based on literature (Smerdon et al., 2016; Hughes et al., 2017), and upon the model framework compiled by the Alberta Geological Survey. Within the corresponding layers of the study's MODFLOW model, these conductivities could be represented in the x- and y-directions, with uniform conductivity in the z-direction (given that each layer is one grid cell thick). While this results in patterns that appear irregular in the 3-D conductivity graphic (Figure 15), representing heterogeneity to the extent

possible is ideal to represent the study area's field conditions most accurately. This is supported by the raw AGS data, which has multiple conductivity values for each layer based on region, as well as publications about formations covered in this study (Dawson et al., 1994; Smerdon et al., 2016; Hughes et al., 2017). The table for the MODFLOW model's input data can be viewed in the Appendix (Table A2).

Three types of boundary conditions were imposed upon the MODFLOW model, done through packages included with the interface: constant heads (CHD), rivers (RIV), and recharge (RCH). The CHD data used was implemented based on observed hydraulic heads in nearby observation or legacy wells. In order to better emulate the variation in heads seen in reality, linear gradients were used for the vast majority of CHD inputs, with hydraulic heads increasing or decreasing in a straight line. The absolute values of these heads were, in part, based on the regional hydraulic head map for the Basal Belly River Formation produced by Brinsky (2014). In addition, heads in areas with lower surface water elevation (northern/downstream portion of the model) were assumed to be at or near surface level for shallow formations such as the Paskapoo.

RIV and RCH data were both taken directly from this study's corresponding SWAT model, so as to keep values constant once the two were coupled. To transfer SWAT's river data into a RIV file, several steps were taken that included joining the MODFLOW grid with the SWAT model's river parameters. The complete process is listed in the Appendix (Workflow 1). Upon completion of this process the river cells can then be imported into MODFLOW. The row and column of the river cells, as well as its stage, depth, thickness of the riverbed, and conductance, are all data required for a successful import.

The RCH data was copied from the SWAT model's "output.hru" file, which contains all output values for the entire model. Throughout the model's building process, different recharge files

were used that gradually increased in detail. Beginning with single, aggregated averages for each subbasin over the entire simulation period, it was evident that more refined data were required for a proper calibration. Yearly data were then introduced, followed by monthly data, which brought the recharge schedule of MODFLOW exactly in line with that of this study's SWAT model. Similar to the process of creating a .RIV file for the study's MODFLOW model, multiple steps were required before importing the data, which are fully described in the Appendix (Workflow 2). Although this recharge data is ignored when the SWAT and MODFLOW models are coupled (Bailey et al., 2016), the data was included in the MODFLOW model as a test of its ability to handle the variable fluxes that would occur in SWAT-MODFLOW.

### *2.2.3. SWAT-MODFLOW Integration*

Before coupling SWAT and MODFLOW, it was required to create linking files, as outlined in step 5 of Figure 11 below. These files serve as a communication bridge between SWAT and MODFLOW, so that data may pass between the two for each time step. The entire process of creating/exporting the correct linking files and coupling the SWAT-MODFLOW model is explained in the tutorial made available by Park and Bailey (2017). Many of the SWAT-MODFLOW input files are prepared using ArcGIS by performing various joins and relates between shapefiles and raster grids, as well as sorting operations in Excel. This yields a set of files that use the same coordinate system (and geo-locations) in both models for easier data transfer.

An essential step in this process is disaggregating SWAT's HRUs (called DHRUs). This separates a given HRU into polygons, which allows for it to be geo-located (Park and Bailey,

2017). This means that for every HRU, there are often far more DHRUs. For this study's 40 HRUs, there are 31047 DHRUs. After the disaggregation of the HRUs, linking files must be created that tell the SWAT-MODFLOW code how many HRUs, DHRUs and MODFLOW grid cells exist in the project. Only then can the DHRUs be linked to their corresponding MODFLOW grid cells for data to be transferred.

Also required are various output files from MODFLOW, which are outlined in the table below:

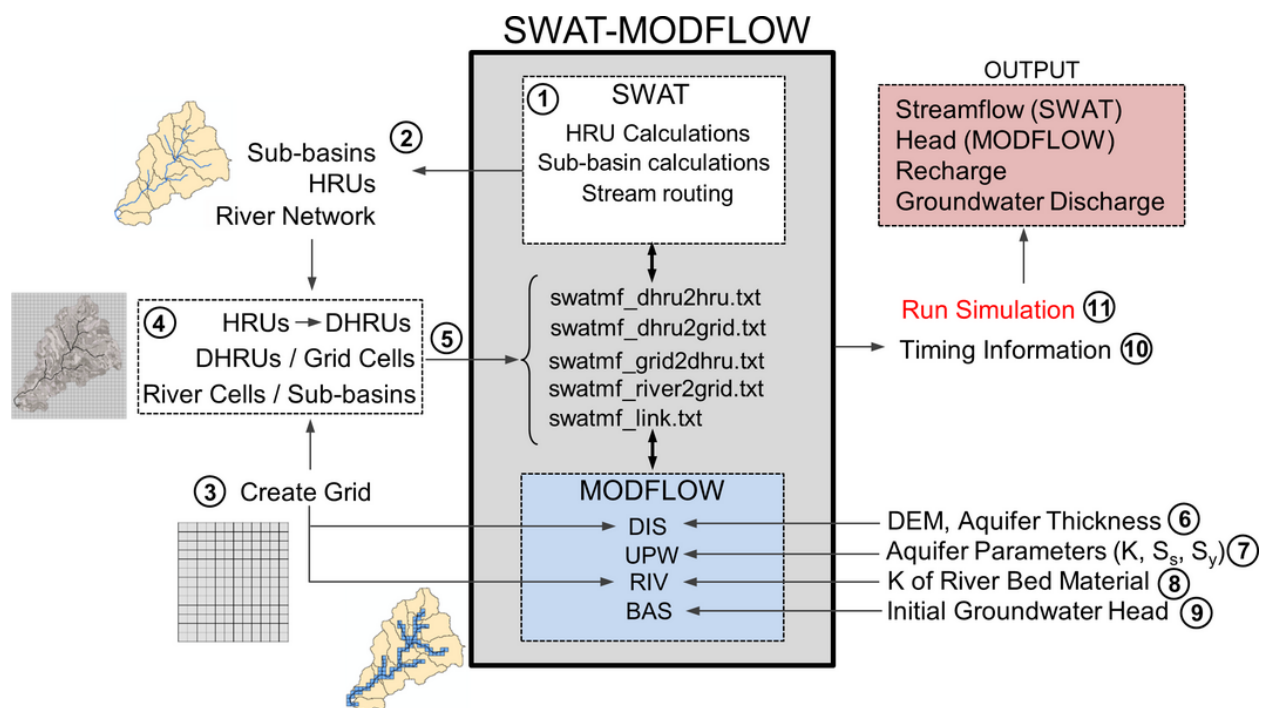


**Figure 11: Schematic of the SWAT-MODFLOW integration process, with the necessary steps and input files outlined (adapted from Park and Bailey, 2017).**

When all required files are compiled into one folder, the SWAT-MODFLOW program can be run. This study uses Bailey's "SWAT\_MODFLOW6.exe" executable, which is an updated version of the original code that was made available after the publication of Bailey et al. (2016).

Although version 2 of this code is publicly available on the SWAT website

(<https://swat.tamu.edu/software/swat-modflow/>, including a tutorial and a SWATMOD-Prep),

the code's author will tailor the executable to fit the needs of the project, such as showing headers for each category (e.g. river cell location and flux rate, as in this study). Depending heavily on the complexity and simulation times of both component models, this SWAT-MODFLOW code may take anywhere from minutes to many hours to run to completion. Many of the MODFLOW input files must be modified before attempting to run SWAT-MODFLOW. Each file has an "identifier number," which helps the code to access it when required. However, some of these identifier numbers overlap with those of the SWAT files, therefore necessitating a change. In the model built in this study, the same protocol was followed as in the SWAT-MODFLOW manual (Park and Bailey, 2017): each identifier number was changed to be 5000 more than the original identifier number (16 would become 5016, etc.). Each corresponding MODFLOW file must then be changed to reflect the new identifier number, which can be done via the "replace" function in Notepad. Careful attention must be paid to the spacing of these identifiers, as MODFLOW is sensitive to placement (it may read "50" instead of "5016" if not spaced properly).

The first trial run with basic SWAT and MODFLOW models was attempted close to the beginning of the study. The purpose of the initial run attempt was to simply become familiarized with the integration process, and occurred before much of the up-to-date data was included in each model. In the case of MODFLOW, a 50 x 50 grid was used, with the formation elevations principally based on literature alone, and the SWAT model did not yet include data for snowfall or other weather parameters. As such, these preliminary models used were not calibrated. Due to the discrepancy between the two models, the coupled model stopped running after 63 simulation days. The second trial run was performed after the completion of the SWAT model, and some refining of the MODFLOW model. This time, the coupling was done to gauge the improvement

after providing one of the models with accurate inputs. As expected, the coupled model ran for more simulation days, before stopping at 164. From this number, it was clear that calibration of both models was essential to the smooth running of SWAT-MODFLOW.

After completely calibrating both models separately (explained further in Section 2.3), the SWAT-MODFLOW model was run a third time. As a result of the MODFLOW model's significant improvement, the coupled model ran for the entire simulation period of 9131 days. The model took roughly six hours to run completely – significantly less time than the initial hypothesis predicted.

Each subsequent run after the third was performed on a more powerful computer, which improved the run time of the coupled model. These runs took slightly less than four hours for a complete simulation, allowing more than one SWAT-MODFLOW run to occur in a day.

## **2.3. Calibration, Validation and Uncertainty Assessment**

### *2.3.1. Importance of Calibration*

Calibration, validation and uncertainty assessment are a set of key steps in evaluating the effectiveness of any model. This is done to ensure that a given model built during a study can be used to simulate and forecast real-world conditions with acceptable accuracy. Generally, calibration is performed by comparing a model's simulated results to a set of observed data from the study area. A separate set of observed data (or the same data points for a different time period) is used after this process as a test, or validation, of the model's simulation ability.

Assuming that the majority of hydro(geo)logic models simulate numerous processes (as in this study), many different model parameters (attributes relating to the simulated physical processes) are required for a realistic representation of field conditions. The changing of these parameters is an essential part of the calibration process, as these changes will be reflected in the performance of the study's model. However, some parameters will affect the model's performance more strongly than others, and so it is important to determine which of these are the most sensitive to change (Abbaspour, 2015).

Any model that represents real-world locations and processes are subject to uncertainties (Abbaspour, 2015). These arise from various sources, including the representation of the conceptual model, the physical processes, and the parameters associated with those processes. As such, the component models used in this study (and by association, the SWAT-MODFLOW model) are not exempt from this. Although the models account for the soils, land use types, hydraulic conductivities and other attributes of the study area, it is impossible for any regional model to fully represent all processes and heterogeneities present in a given area.

Another source of calibration uncertainty lies in parameter non-uniqueness, a term used to explain that similar calibration results are possible with widely differing parameter value combinations (Abbaspour, 2015). It is commonly encountered when performing inverse modelling as a calibration method, in which scientists use the outputs of a model to make decisions about parameter changes for future iterations (Abbaspour et al., 1997). As such, the more parameters that a model simulates, the more uncertainty is potentially introduced.

The primary method used to limit non-uniqueness in this study (with respect to both component models) was to base the calibrated parameter values on measured or published data wherever possible. As will be explained further in Sections 2.3.2 and 2.3.3, these sources include studies

by Smerdon et al. (2016) and Hughes et al. (2017), as well as public weather data (see Table A2) and guidelines set within the documentation for the SWAT software (Arnold et al., 2012).

### 2.3.2. SWAT Calibration

Within the SWAT software, the model runs successfully for the simulated duration of 25 years in minimal time (a matter of seconds). For the optimal run, a warm-up period of three years was used, bringing the first data year to 1986. As explained before, the HRUs calculate outputs for each subbasin at each daily time step, although the model was manually set to display aggregated monthly outputs in this study. The model was then calibrated by using observed monthly stream flow data at two hydrometric stations within the study area (Flow\_119\_1 and Flow\_118\_24). This was accomplished with SWAT-CUP, a program designed for the efficient calibration of SWAT models (Abbaspour, 2015; Texas A & M, 2017). Various calibration techniques are available to use with the interface, and this study uses the SUFI2 (Sequential Uncertainty Fitting) algorithm (Abbaspour et al., 2007; Faramarzi et al., 2009). SWAT-CUP is a calibration tool that works by performing sensitivity analyses to determine which parameters most affect the SWAT run results. Further to this, the SUFI2 algorithm performs Latin Hypercube sampling for user defined parameter ranges and calculates possible outputs within a 95% confidence interval (95PPU) (Abbaspour, 2015). The SUFI2 program compares the model's simulated discharge to the observed data using a variety of statistics, including  $R^2$  and  $bR^2$ . A model's  $R^2$ , or coefficient of determination, relates to how well the simulated data trend replicates the observed trend (Faramarzi et al., 2015). The primary factor observed in this study, however, is  $bR^2$ , which takes both trend and closeness to observed results into account, and is calculated by multiplying  $R^2$  by  $b$ , or the slope of the regression line between observed and simulated data (Faramarzi et al., 2015). Ranging from 0 to 1, a higher value indicates a better-calibrated model. However, since it

is impossible to reach a  $bR^2$  value of 1 other than by over-calibrating, values are considered acceptable once they start to plateau after many iterations (in the range of 0.5 – 0.7). Also important are the p-factor and r-factor of the results. An iteration's p-factor, measured on a scale of 0 to 1, considers how well the best simulation stays within the 95% confidence interval (Abbaspour, 2015a) that is due to the parameters' uncertainty range. As such, a p-factor closer to 1 is ideal. The r-factor represents the range of simulated results. As a well-calibrated model should simulate data within a range close to the observed results, a smaller r-factor is ideal, with a result under 1 considered to be passable.

Within the study area, two hydrometric stations are present, which are situated in subbasins 1 (station 119\_1) and 24 (station 118\_24) and are used as calibration points for the SWAT-CUP process (Figure 8). These hydrometric stations yield river discharge data on a monthly basis, which is used to calibrate against SWAT's simulated river discharge at the previously mentioned subbasins. In total, we evaluated 45 parameters of the SWAT model (see Table A4), with 100 simulations per iteration. Due to the proximity of sub-basin 24 to the Rocky Mountains, it was treated as its own system, without further regionalization of the parameters. Snow-related parameters were also added as a variable, due to their potential sensitivity (see Table A4). Between iterations, widening and narrowing ranges of certain parameters within a physically meaningful range resulted in changes to the accuracy of calibration. The parameter ranges used within this study were based on those in the SWAT input-output documentation (Arnold et al., 2012), as well as those of the project's soils database (see Table A2 for data source). When the simulated values for river discharges are close to matching the observed values for each stream gauge (yielding  $bR^2$ , p-factor and r-factor values within the desirable range discussed above) for the entire simulation period, the SWAT model is considered to be well-calibrated. As more

recent historical data is generally accepted to be more reliable (and was of greater interest due to the planned forecasting scenarios), the SWAT model was calibrated for the 1996-2007 period, with model validation occurring for the 1986-1995 period.

### *2.3.3. MODFLOW Calibration*

The project setup and initial runs were carried out under steady-state (SS) conditions, to establish an initial condition for subsequent runs. This was done so that the initial heads file (.HDS) could be used to run transient simulations. The initial SS condition model had a computational time of less than a minute. After this initial run, variable recharge data was added to the model (in the increments explained above), with the corresponding SWAT model as its source. This recharge data was subdivided by SWAT subbasin, and was added to the top layer of the MODFLOW model in its corresponding location (see Figure 8). As expected, the computational time increased as more detailed recharge data was introduced to the model. When monthly values were introduced for each subbasin and run under TR conditions, the total run-time was just over thirty minutes.

To allow for a full run of the MODFLOW model (and, by extension, the SWAT-MODFLOW model), some controls under the “Run” menu of Visual MODFLOW had to be changed from their default values. In particular, the “Maximum Outer Iterations” value, found under “Solver,” had to be increased to allow for more than 100 iterations per time step. Although the most outer iterations required for any single time step was 112 at the 2652<sup>nd</sup> simulation day (with the vast majority of time steps far under this value), the “Maximum Outer Iterations” value was changed to 1000 to account for possible increases to the iteration number when the model was coupled with SWAT.

To ensure the accuracy of the GW flow model, wells from the Alberta Water Well Database were input as calibration points. Though publicly available, only two wells with hydraulic head data were found through the Alberta Water Well Database or GOWN (Groundwater Observation Well Network) for the study area. However, the Alberta Geological Survey and Alberta Groundwater have maintained records of many more data points in the area, with static water level measurements taken primarily in conjunction with the drilling of oil and gas wells (Figure 12). These water levels were converted to hydraulic head data by subtracting from the wellheads' ground elevations, with screen elevations assumed to be at the bottom of each well. Ultimately, 377 legacy wells were available within the MODFLOW modeled area, with many of those falling directly within the Little Smoky River watershed. Due to the number of data points, calibration was limited to well measurements taken in the last five years of the simulation period (January 2003 – December 2007).

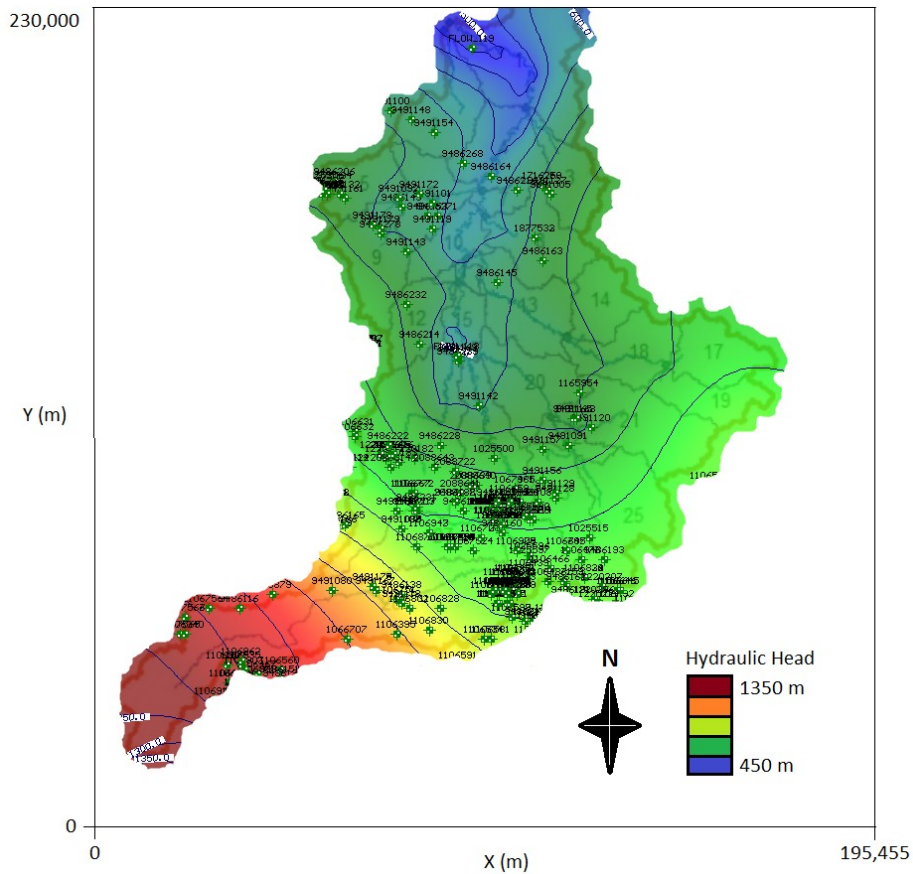


**Figure 12: A colored contour map of hydraulic head for the Little Smoky River watershed, produced by Visual MODFLOW. The hydraulic head roughly follows the area’s topography, with higher heads found in the upstream regions of the area. Each small number on the map represents a calibration well within the Little Smoky River watershed.**

In addition to the observation wells mentioned above, the two stream monitoring gauges within the study area (Flow\_118 and Flow\_119) were also input as continuous calibration points (data for the entire simulation period), bringing the total to 379. Although the flow rates at each point are commonly used, monthly river stage was used instead for this component (provided by Alberta Environment and Parks), due to the MODFLOW model’s primary calibration parameter being hydraulic head.

To evaluate the overall representation of observed data, various statistics were used, similar to the calibration process of the SWAT model. The principal statistic used was the simulation's normalized root mean square error (RMS), which evaluates a simulated dataset's overall closeness to the observed dataset (Hyndman and Koehler, 2006). Generally given as a percentage, values closer to 0% indicate less deviation from the observed dataset. The model was also calibrated using the average correlation coefficient, a value that evaluates the linear relationship between two variables (Pearson, 1895), which in the case of this study are observed head and simulated head. Ranging from -1 to 1, a value closer to 1 represents a better correlation. The vast number of observation points and Visual MODFLOW's GUI allowed the pinpointing of locations with larger hydraulic head discrepancies, which facilitated parameter adjustment for future iterations. Many parameters and boundary conditions can be changed to achieve satisfactory calibration/validation results, including specific storage, specific yield and hydraulic head-related boundaries, but the key parameter in many MODFLOW models is the hydraulic conductivity of the layers. As these values need to be changed largely based on region, it is therefore important that the values of hydraulic conductivity in a given model be based on those found in the corresponding subsurface units to the extent possible. To that end, the calibrated values used in this study were kept within the ranges found in studies such as those by Hughes et al. (2017) and Smerdon et al. (2016).

#### **2.4. Scenario Analysis**

In order to more fully understand the WFE nexus and its potential influences, different scenarios were applied to the coupled SWAT-MODFLOW model to determine the possible range of

effects that could occur in the real world. Two potentially significant contributors to hydrological change in this basin are water well pumping and climate change. For this purpose, climate data simulated by five General Circulation Models (GCMs) were used (Table 1), which are climate change tools based on physical processes (IPCC, 2014). Although GCMs simulate processes associated with climate and weather changes at a large spatial scale (some with resolutions of roughly 10 km), their output data must be downscaled for application to smaller-scale watersheds and local climates (Chen et al., 2011). A widely used method to accomplish this task is by establishing an empirical link between the selected GCM(s) and observed data for the historical period from the study area, known as the change factor approach (Chen et al., 2011). By using this method, the formulations obtained for the historical period can then be applied for future projections. The strength of GCMs lies in their ability to forecast scenarios with different assumptions for the future, known as Representative Concentration Pathways, or RCPs (van Vuuren et al., 2011). Based on the projected emissions of greenhouse gases, the most widely used of these RCPs are RCP2.6 (the most environmentally optimistic scenario) and RCP8.5 (the heaviest greenhouse gas emission scenario), as seen in Figure 13 below. Each produces distinct model outputs, and dedicated climate change studies use these to obtain the widest range of possible climate outcomes.

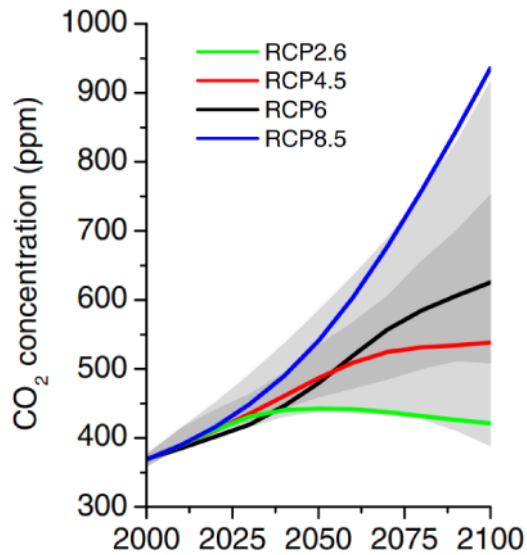


**Figure 13: Diagram of carbon dioxide concentrations when considered under various climate change scenarios, including RCP2.6 and RCP8.5 (adapted from van Vuuren et al., 2011).**

As a key objective of this study was to evaluate the SWAT-MODFLOW tool’s ability to simulate a watershed under the effects of both natural and human influences, the results for three scenarios (in addition to the base scenario) will be presented, with the **first** focusing solely on the effects of pumping, with 21 wells installed proximal to or within the study area (found within the same areas as the legacy boreholes used for calibration), pumping at a rate of 468 m<sup>3</sup>/d for six months of each simulation year. These rates were proposed by Encana, an Albertan energy company with hydraulic stimulation operations nearby the study area. The **second** coupled scenario will include climate change and no pumping, averaging the results for five distinct GCMs (Can\_ESM2, CCSM4, CNRM\_CM5, CSIRO-MK3, and MIROC5) from the Pacific Climate Impact Consortium (PCIC, <https://www.pacificclimate.org/data>) under the RCP8.5 (high carbon emissions) scenario (Table 1). The **third** pushes the SWAT-MODFLOW model to the extreme, applying the climate change scenario described above and increasing the pumping rate of the first scenario’s wells by an order of magnitude (4680 m<sup>3</sup>/d). These GCM models (Table 1)

were downscaled to match the observed interval of the reference period (1983-2007) to establish an empirical relationship between them and study’s model. This relationship is then used to project data for the future scenarios, resulting in a simulation period of 25 years (2010-2034), similar to the historical model.

**Table 1: General information of selected GCMs and scenarios available from PCIC.**

Acronym	Country	Source
CanESM2	Canada	Canadian Centre for Climate Modeling and Analysis
CCSM4	United States	National Center for Atmospheric Research
CNRM-CM5	France	Centre National de Recherches Meteorologiques/Centre Europeen de Recherche et Formation Avancees en Calcul Scientifique
CSIRO-MK3	Australia	Commonwealth Scientific and Industrial Research Organization in collaboration with the Queensland Climate Change Centre of Excellence
MIROC5	Japan	Meteorological Research Institute

The pumping wells were primarily included in the downstream portion of the MODFLOW component, once the topography begins to level out (Figure 20). This was done to reflect more realistic placement of the wells in the agricultural and deciduous forest-dominated areas where energy operations are more common, as opposed to a more widely distributed network. The terrain in the upstream portion of the watershed, as described in Sections 2.1 and 2.2, approaches the foothills of the Rocky Mountains, which means that uneven and highly varied elevation is common. The boundary conditions and physical parameters of the MODFLOW model remained unchanged apart from the increased pumping rates, as the subsurface properties are assumed to

be constant on a scale of decades. Furthermore, the precipitation is replaced by the new climate change-affected values of the SWAT model.

### **3. RESULTS AND DISCUSSION**

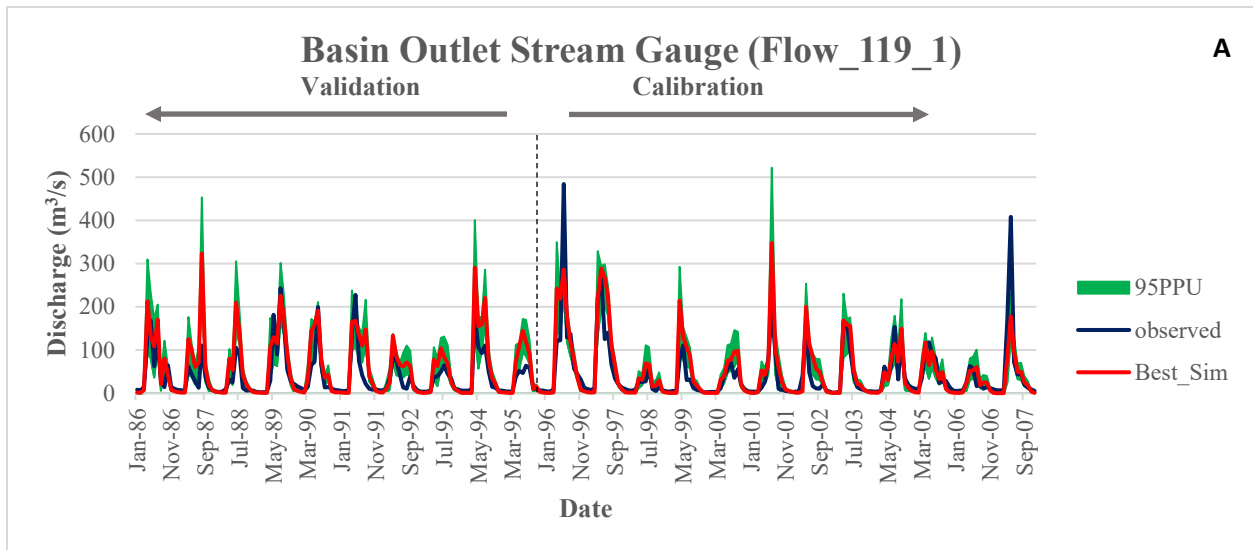
#### **3.1. Parameter Sensitivity Results**

##### *3.1.1. SWAT*

With a preliminary SWAT run prior to calibration, the simulated results overestimated the river's peak flows when compared to the observed values. For calibration purposes, a total of 21 physical parameters sensitive to river discharge were selected from literature (Faramarzi et al., 2015). The parameters were further regionalized to capture a higher degree of spatial variability due to land use, soil, and hydrologic conditions for a total of 45 sensitive parameters. From these, a one-at-a-time style sensitivity analysis was performed, evaluating the model's reactions to changes in single parameters. While changing the 45 parameters through the calibration procedure using the SUFI2 algorithm in SWAT-CUP, some naturally caused greater changes in the overall model performance. The addition of elevation bands (PLAPS and TLAPS, allowing multiple temperature and precipitation values to capture the effects of orographic changes within a subbasin) improved the overall calibration performance, particularly in Subbasin 24, which was treated as its own system. Allowing for more water capacity in the soil (SOL\_AWC), and less runoff (CN2) also brought down the overestimated peak flows. The final values were kept within the range provided by the model's soil input data, with a maximum water capacity of 0.333 mm H<sub>2</sub>O and the curve number decreased by 44%. To further cement this peak flow reduction, the soils' hydraulic conductivity values were increased as well. In addition to the above, snow-

related parameters (.sno) were altered so that the model’s snowfall and snowmelt simulations occurred in the correct temperature range (-5 to 5 °C). A complete list of the parameters used, and their initial and final value ranges, can be viewed in the Appendix (Figure A4).

As mentioned in Section 2.3, the study’s SWAT model was calibrated using the SUFI2 algorithm of the SWAT-CUP software, using historical data from two stream gauges within the Little Smoky River Watershed. While initially calibrating to optimize the  $bR^2$  value, the p-factor, r-factor and  $R^2$  of the model were also statistics that were prioritized throughout the process. In Figure 14, the final results can be seen for both gauges. The data is shown on a monthly basis, which clearly outlines the contrast between the peak flows of the summer and the low flows of the winter months. By changing the parameters as described above and in Section 2.3.1 and 2.3.2, the simulated overprediction of peak stream discharge was mitigated. However, the SWAT simulation consistently under-predicts river discharge in low-flow periods (winter months), even after calibration. We believe that this is due to the model’s limited ability to take GW discharge into account, an issue that the study’s corresponding MODFLOW model remedies.



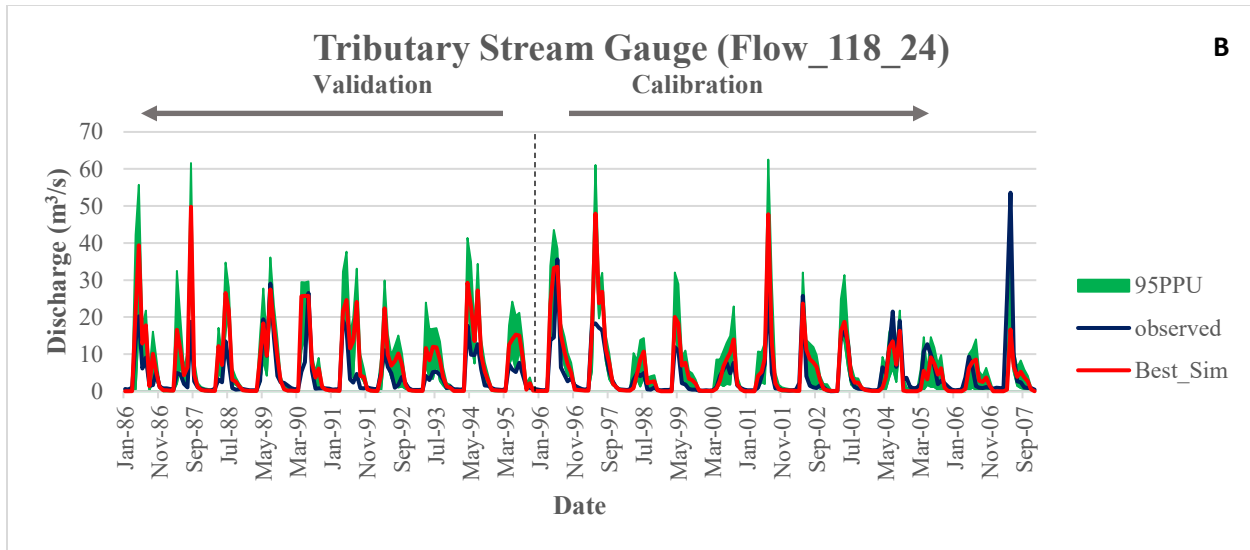


**Figure 14: 95ppu graphs for both calibration points in the Little Smoky River Watershed over the entire historical simulation period. Significantly higher flow values were observed and simulated at the watershed’s outlet (A) than in the measured tributary (B).**

Validation of the model was performed by comparing the simulation to observed data for the 1986-1995 period. Overall, the model follows very similar trends, with the peak flows of some years being slightly overpredicted, and the low flows of the winter months falling to zero for most simulation years. Apart from not being the primary focus of calibration, the discrepancies between the simulated and observed curves for the validated timespan of the SWAT model may be due to the short period of calibration/validation. With a longer period, the model may have had improved responses to extreme events such as droughts or floods, due to a greater possibility of these events occurring over longer timespans. The final summary statistics for the SWAT component’s calibration and validation process at each stream gauge can be viewed below (Table 2). As described in Section 2.3, these factors measure not only the SWAT simulation’s fit to the observed trend, but its closeness to that trend as well. Due to this study’s focus on applying

new scenarios to a coupled SWAT-MODFLOW model, the summary statistics below were taken to be satisfactory for the purposes of coupling with the MODFLOW model.

**Table 2: Final combined summary statistics for the calibrated and validated SWAT model. Initial refers to prior to calibration.**

Hydrometric Station	Drainage Area (km <sup>2</sup> )	p-factor	r-factor	R <sup>2</sup>	Initial R <sup>2</sup>	bR <sup>2</sup>	Initial bR <sup>2</sup>
Flow_119_1 (Outlet)	11140	0.44	0.65	0.67	0.29	0.6282	0.0521
Flow_118_24 (Tributary)	1041	0.52	0.85	0.58	0.46	0.5685	0.3774

### 3.1.2. MODFLOW

As outlined in Section 2.5, the model’s hydraulic head output was calibrated using 379 points, consisting of water observation wells, legacy boreholes and the two stream gauges used to calibrate the SWAT model. Throughout the calibration process, it was found that the most sensitive parameter of the model was hydraulic conductivity. While maintaining values that were realistic in the field (Hughes et al., 2017) and true to the data provided by the AGS, the conductivities were modified to create heterogeneous layers (see Section 2.3.3).

At the onset of MODFLOW calibration, the thin, pinching-out layers in the model’s northern end (seen in Figure 10) caused problems for vertical flow. Since the simulated water could not flow down through the cells effectively, this resulted in areas where hydraulic heads would build to be significantly higher than what can be observed (or is realistic). Introducing Constant Head boundary conditions (CHB) on the perimeter of the MODFLOW modelled area helped to bring the model’s hydraulic heads down to a more realistic range. These CHBs were based primarily on the area’s ground elevation, and on the hydraulic head map of Brinsky (2014) for deeper formations such as the Belly River/Wapiti. Care was taken to not include CHBs in the model

area that would be directly coupled with SWAT, allowing the model's hydraulic head to fluctuate as needed.

Apart from imposing CHBs proximal to the study area, changing the hydraulic conductivity of each layer was another significant factor in the model's successful calibration. While remaining faithful to the realistic ranges outlined by literature (Dawson et al., 1994; Smerdon et al., 2016; Hughes et al., 2017), each MODFLOW layer was given multiple hydraulic conductivity values so as to simulate geological units that were heterogeneous in two dimensions (x and y). These layers could not be vertically heterogeneous due to each being a single grid cell thick, regardless of the actual thickness of the cells. Figure 15 below displays the distribution of hydraulic conductivities in the study's MODFLOW model.

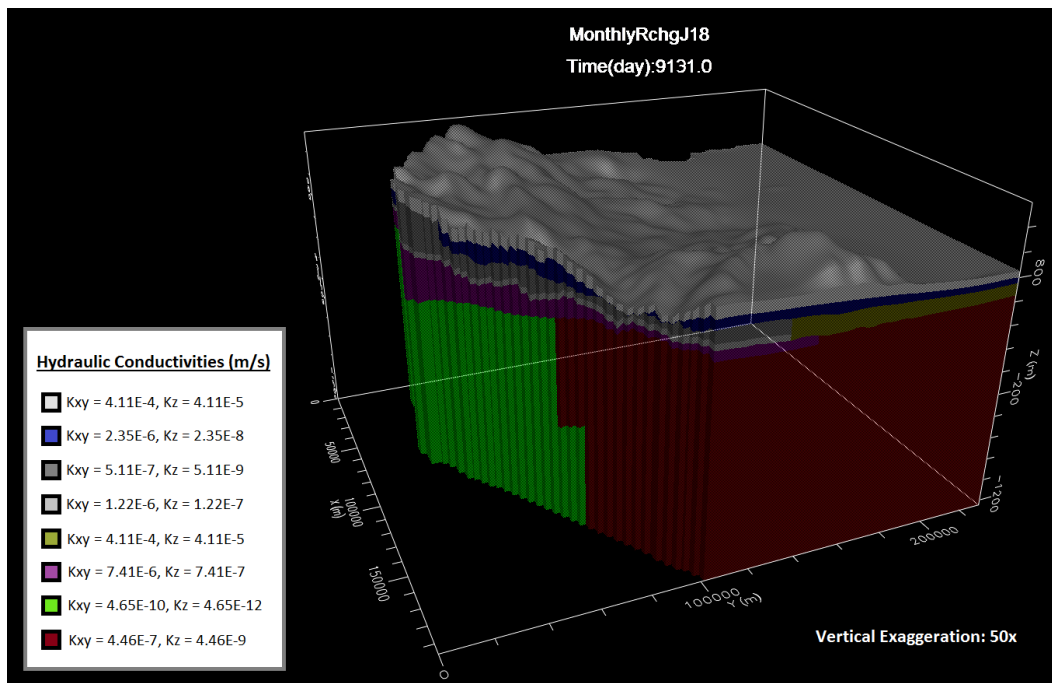


**Figure 15: 3-D diagram of the study's MODFLOW model, with each color representing the hydraulic conductivity found at that point. Many of the model's layers have more than one conductivity value.**

Although calibration initially began with single-value recharge data for each subbasin, this was quickly changed to yearly, and finally monthly data. As more detailed recharge data was added from the SWAT model to the MODFLOW model over time, the results of the calibration for each time step improved, marking the model's positive reaction to more variable recharge. This proved that, even though these specific recharge values would be replaced by those of the SWAT model, the MODFLOW model performs well under the same conditions as are used in the SWAT model.

The calibration's progress was measured by comparing the simulated hydraulic heads to observed hydraulic heads (Figure 16 and Table 3), with several commonly used summary statistics for each time step including the normalized RMS, the correlation coefficient, the standard error and the residual mean. For most of these statistics, smaller values point toward a more accurate calibration (with the exception of the correlation coefficient, where values closer to 1 indicate a better fit).

An average correlation coefficient of 0.956 and an averaged normalized RMS of 6.506% were observed after the calibration process for MODFLOW. These values indicate that the simulation represent most of the observation points well. Some outlying points remain, with a maximum residual observed of -155.379 m, but the majority of data points such as this were located more than 10 km from the area covered by the study's SWAT (and, by association, SWAT-MODFLOW) model. Additional calibration would be required for a model that directly influences policymaking, but the results were deemed satisfactory for a model of this regional scale, whose purpose is to support the testing of various coupled scenarios.

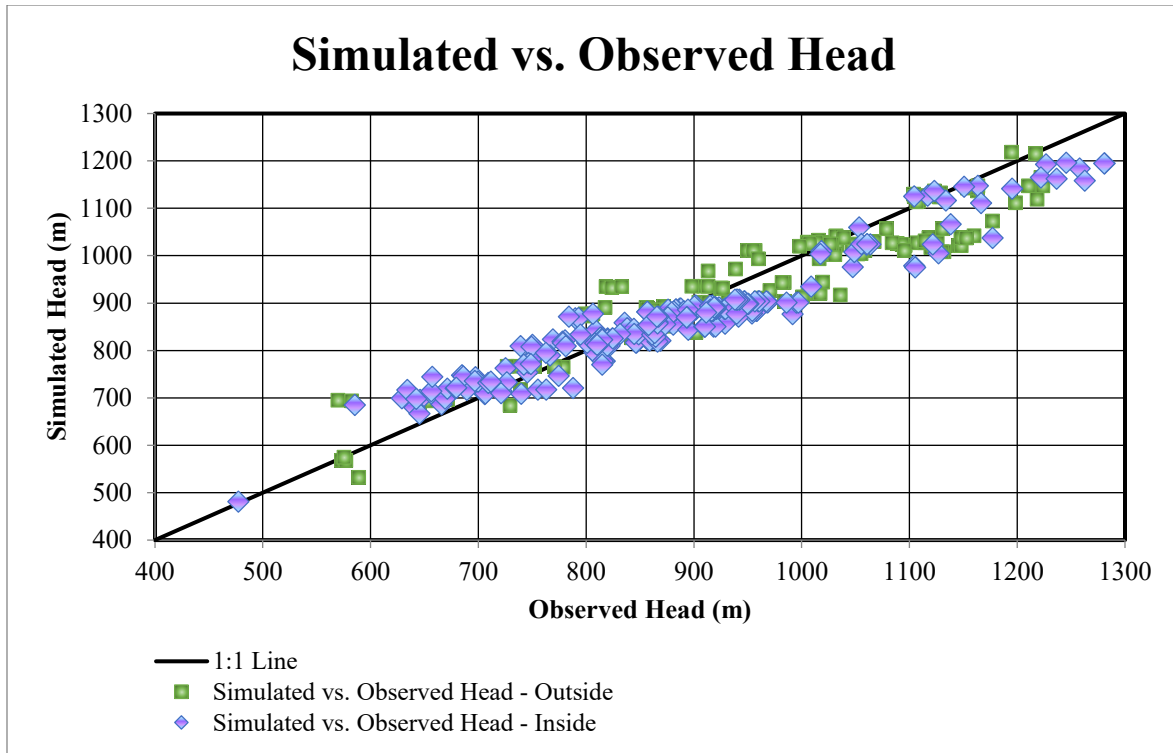


**Figure 16: Calibration graph for the MODFLOW component, comparing simulated hydraulic head values to the observed hydraulic head values at each observation well outside and inside the Little Smoky River watershed.**

**Table 3: Summary statistics for the MODFLOW component. Although similar graphs can be displayed throughout the simulation period, the Normalized RMS remains relatively constant between 6% and 7%.**

<b>MODFLOW Summary Statistics</b>	<b>Total</b>	<b>Inside Watershed</b>	<b>Outside Watershed</b>
Number of Data Points	379	238	141
Max. Residual (m)	-139.801	-139.801	-128.471
Min. Residual (m)	0.134	-0.038	0.511
Residual Mean (m)	-16.746	-15.369	-18.442
Normalized RMS (%)	6.506	5.743	8.617
Correlation Coefficient	0.956	0.961	0.942

## 3.2. SWAT-MODFLOW Runs and Results

### 3.2.1. Results and Outputs

After calibration of the component models, the study's SWAT-MODFLOW model ran for the entire simulation period of 25 years (1983-2007), with run times varying from 4 to 6 hours depending on the processing power of the machine on which it is run. After each SWAT-MODFLOW run, several output files are produced, which have been listed in the table below (Table 4):

**Table 4: List of SWAT-MODFLOW outputs and their contents (modified from Beets, 2016).**

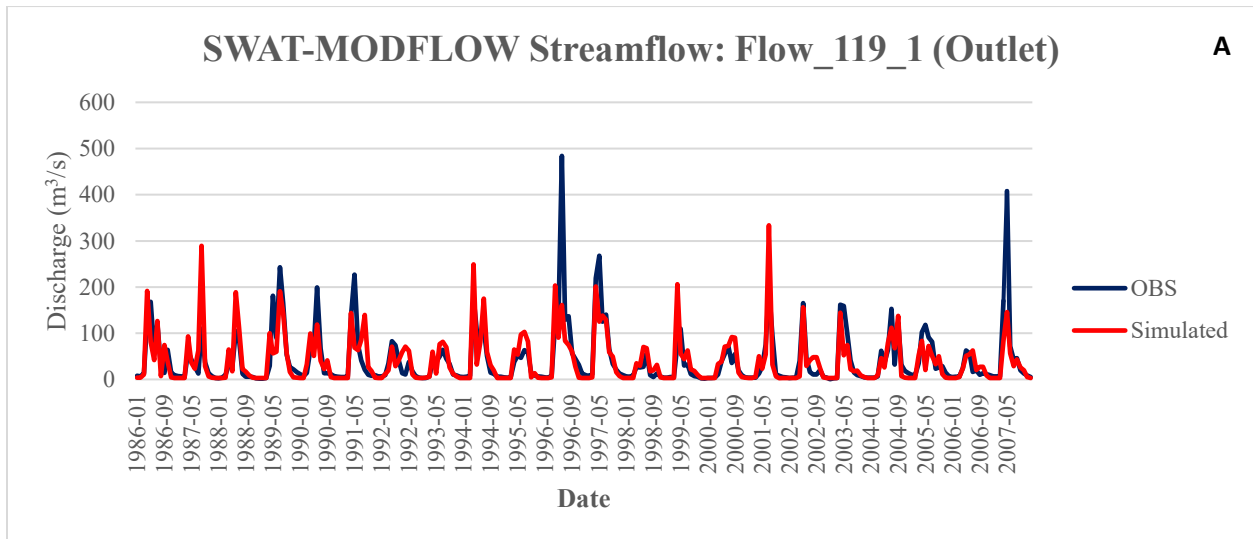
Name	Content
<b>swatmf_out_MF_gwsw</b>	GW-SW exchange (m <sup>3</sup> /day) for each MODFLOW River cell. Positive values are for river water entering the GW system, and negative values are for GW entering the river.
<b>swatmf_out_MF_recharge</b>	Recharge (m <sup>3</sup> /day) to the water table for each grid cell, for the day. The cell values are printed as a grid, at each daily time step of the simulation.
<b>swatmf_out_MF_riverstage</b>	MODFLOW river stage (m) for each river cell, listed in order of the river cell ID.
<b>swatmf_out_SWAT_channel</b>	Channel depth (m) of each subbasin stream, listed in order of subbasin # across the columns (i.e. each row in the file is one simulation day).
<b>swatmf_out_SWAT_gwsw</b>	Exchange (m <sup>3</sup> /day) for each subbasin, listed in order of subbasin # (1 to ...) for the day. Positive values are for GW entering the river, and negative values are for river water entering the aquifer.

**swatmf\_out\_SWAT\_recharge**

Deep percolation (mm) calculated for each HRU. The values are listed in order of HRU # (1 to ...) for the day and are printed out for each day of the simulation.

### 3.2.2. Streamflow and GW-SW Exchange

To ensure the accuracy of the tool, the stream discharge results for the SWAT-MODFLOW model were compared to the observed streamflow data used to calibrate the project's SWAT model. Although the GW discharge in the winter months did not increase as predicted, the simulated streamflow of the coupled model had similar accuracy to that of the SWAT model by itself at both stream gauges (Figure 17A and B). The  $R^2$  statistic at Flow\_119\_1 and Flow\_118\_24 for this run of SWAT-MODFLOW were 0.536 and 0.484 respectively.



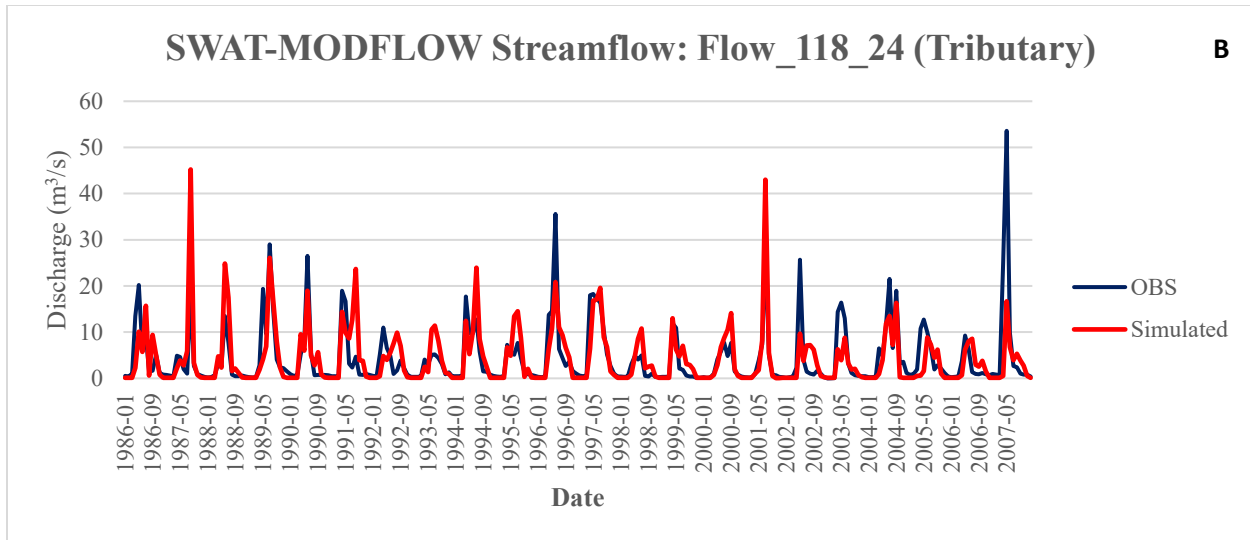


**Figure 17: Simulated vs. observed streamflow for the watershed’s two stream gauges (Flow\_119\_1 (A) and Flow\_118\_24 (B)). The results are similar to those of the calibrated SWAT model, indicating a cooperative GW input from the MODFLOW component.**

A key output of the SWAT-MODFLOW model is detailed GW-SW interaction for each MODFLOW river cell in the watershed, found in the file “swatmf\_out\_MF\_gwsw.” At each time step, a discharge value is given for every MODFLOW river grid cell, with flux values recorded with respect to the GW system (Figure 18). As such, positive values indicate recharge into the GW system, and negative values indicate discharge from aquifers into the watershed’s streams (Park and Bailey, 2017). For nearly every river cell in the study area, discharge from the aquifer was recorded, but the magnitude varies significantly. These variations are based on a multitude of factors, but primarily owe to the hydraulic head found at each of these river cells. The hydraulic conductivity of the aquifers can also affect the simulated discharge, especially in areas of variable conductivity. Flowrate deviations from the base average (Figure 18) for select months are given in Figure 19.

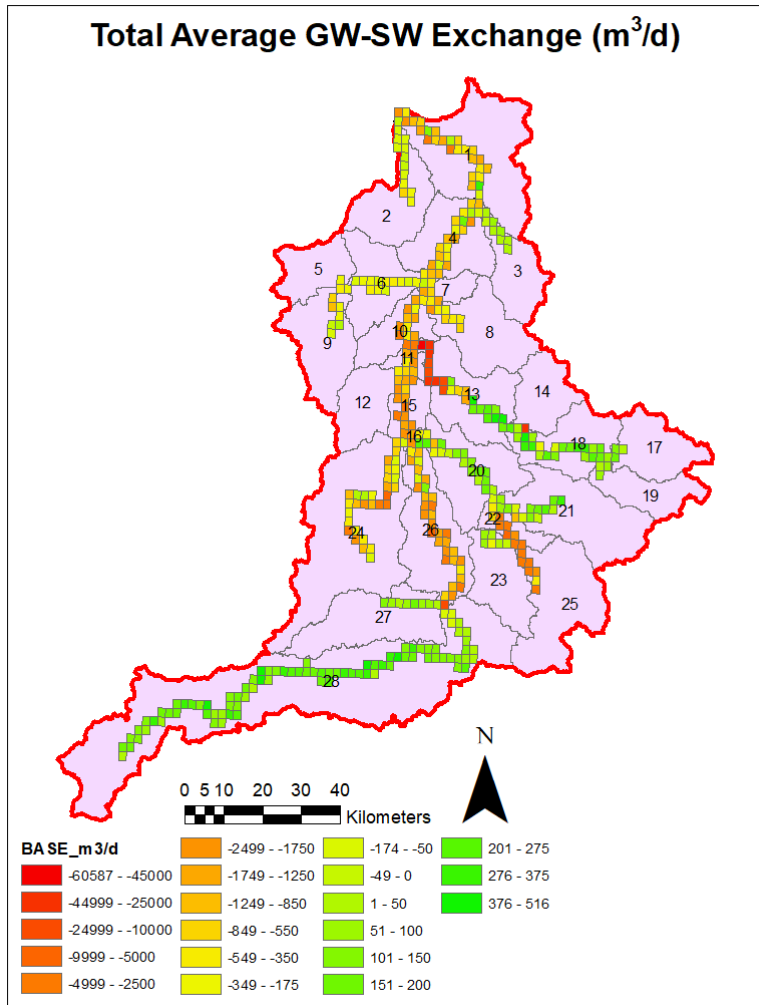


**Figure 18: Plan view map of the Little Smoky River watershed, with long-term (1986-2007) average annual GW-SW exchanges displayed for each MODFLOW river grid cell. Positive values indicate recharge from the river into the GW system, whereas negative values indicate discharge from the GW system into the river.**

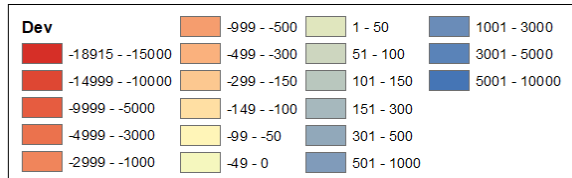
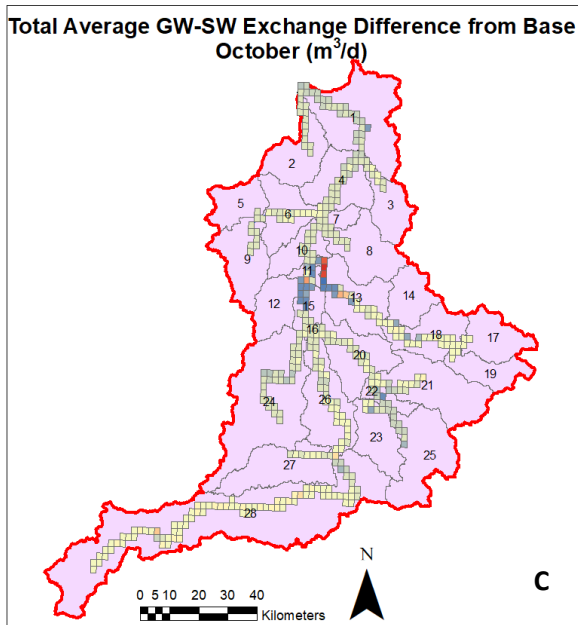
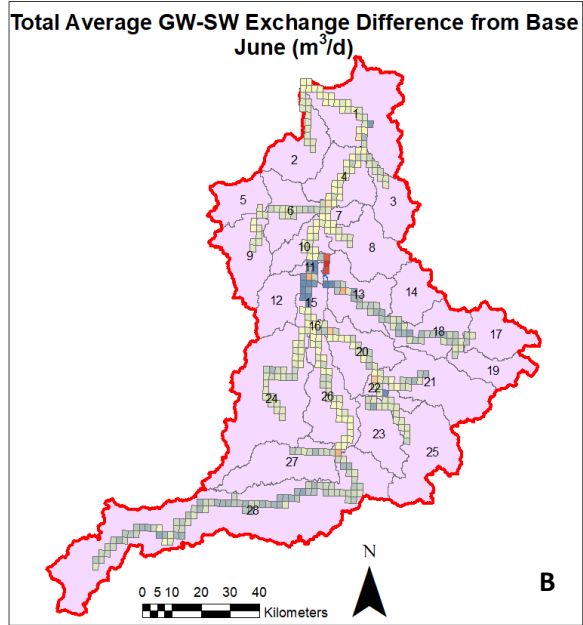
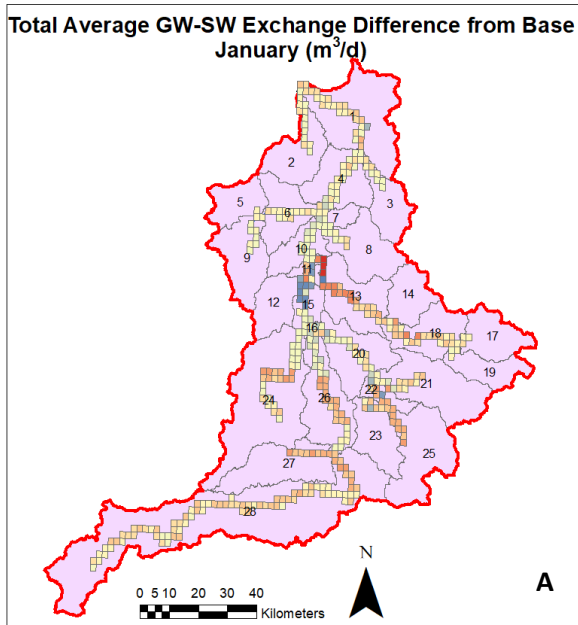


**Figure 19: Long-term (1986-2007) average monthly GW-SW exchange differences from the overall (Figure 18) for each MODFLOW river cell, in the months of January (A), June (B), and October (C). Dev (m<sup>3</sup>/d) = month (m<sup>3</sup>/d) -year (m<sup>3</sup>/d).**

### *3.2.3. GW-SW Interaction Patterns*

The simulated GW-SW exchange flux values range considerably and are highly dependent on location, but are primarily negative, which indicates discharge from the area's aquifers. Positive values can reach into the hundreds of cubic meters per day (to a maximum of 794 m<sup>3</sup>/d per grid cell), whereas negative values can, in many grid cells and time steps, reach into the tens of thousands of cubic meters per day (to -62,479 m<sup>3</sup>/d per grid cell, discussed further in Section 4.1). This indicates a significant interaction occurring between the GW and SW systems of this watershed and will prove useful for providing dynamic data to future GW-SW projections using the workflows applied here.

In each of the GW-SW exchange diagrams shown above (Figure 18, Figures 19A, B and C), local patterns of interaction can be observed. Although overall exchange trends remain fairly constant throughout the simulation period, the southern (upstream) portion of the river shows the most pronounced fluctuation between the wet and dry months, with higher relative discharge from the aquifer occurring during January, and less aquifer discharge (more stream seepage in subbasins 13-14, 17-22, 27-28) taking place in June. In addition, the tributary found within Subbasin 13 of the study area consistently has the highest flow rates observed. The reason for these recorded patterns may be due to the area's bedrock strata: more formations pinch out and outcrop to the north, so the changes in flow patterns may be partially caused by the hydraulic conductivity of layers that are close to the surface.

### *3.2.4. Model Outputs Discussion*

The outputs produced by the coupled tool fall within the acceptable range of values for the study area, as the simulated streamflow values produced by the coupled SWAT-MODFLOW model

faithfully reproduce the results of the study's calibrated SWAT model (Figures 14A and B, 17A and B). With regards to the GW-SW exchange flow rates, even MODFLOW grid cells with discharge values of over 50,000 m<sup>3</sup>/d convert to m<sup>3</sup>/s values of less than 1, which are minor in comparison to the river discharges in the area, particularly at the outlet gauge. Furthermore, it is possible that the MODFLOW model's grid cell size contributed to these values, as each cell's discharge is output for an area of roughly 4 km<sup>2</sup>. Discharge from the aquifers into the stream network was observed in most grid cells throughout the year, with the highest fluctuation in the exchange values seen in the southern subbasins (subbasins 13-28). Reflecting the seasonal fluctuation present in the study area, lower values of aquifer recharge (relatively higher discharge) were observed in the winter months, with these values increasing in conjunction with the snowmelt and higher river discharge of spring and summer (Figures 19A and B).

### *3.2.5. Model Application: Water-Food-Energy Nexus*

As there is pronounced energy activity in the study area, it was important to take water extraction by wells into account within the model built here. To test the effects that simulated water pumping wells would have on the flux of GW and SW in the watershed, a batch of 21 wells was first included in the MODFLOW component (Figure 20), with pumping rates of 468 m<sup>3</sup>/d. Screens for each well were inserted in one of the two aquifers in the study area: either the Paskapoo Fm., or the basal Belly River/Wapiti Fm. The Paskapoo and Basal Belly River have proven aquifer potential in the study area (Hughes et al., 2017), and have already had water wells drilled within them in other parts of the province. The pumping rate, taken from an example water extraction well drilled by Encana in the Fox Creek area, was active for half of each year after the 3-year warm-up period, beginning at the start of each simulation year. After performing

a run within MODFLOW itself to produce additional pumping-influenced outputs, the updated model was then used to couple with SWAT.

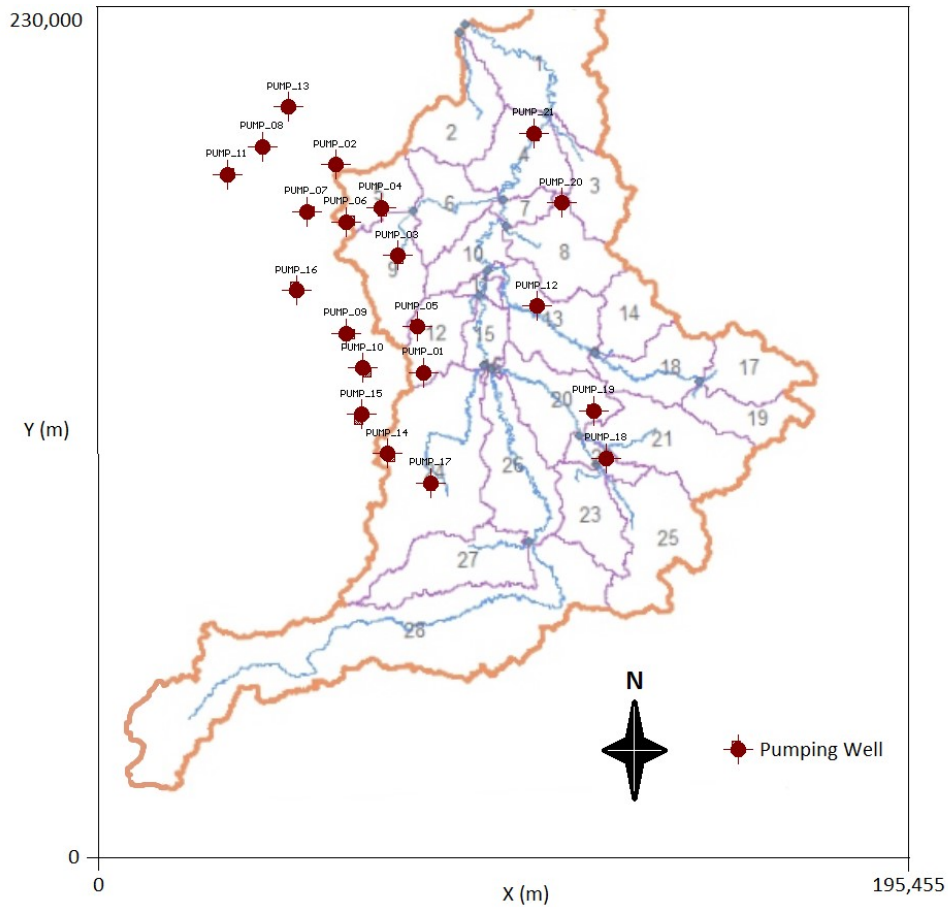


**Figure 20: Map of the Little Smoky River watershed within the MODFLOW modelled area, with simulated pumping well locations included. Each well is proximal to or within the study area, with 16 of the 21 pumping wells located in the downstream portion of the modelled area.**

A coupled simulation of stream flow using SWAT-MODFLOW and including the pumping schedule mentioned above took more time, with the run time increasing from 4 hours to 5 hours. As expected, the hydraulic heads in the regions with wells decrease, with a difference of up to 5 meters of drawdown observed in comparison with the SWAT-MODFLOW model without pumping wells. In addition, the influence of water well pumping had an effect on the observed

cell-by-cell GW-SW flow rates. On average, the aquifer discharge rate decreased, with the simulated flow rate changing from  $-1294 \text{ m}^3/\text{d}$  to  $-1261 \text{ m}^3/\text{d}$ . This discharge rate decreased in 329 of the 405 river cells, and the maximum observed decrease in discharge was  $937.8 \text{ m}^3/\text{d}$ .

The GW-SW interaction change observed is likely due to the fact that as water is extracted from the subsurface, less of the remaining water is available to provide baseflow to the study area's rivers. Depending on the rate and schedule of pumping (including the number of pumping wells), these results show that the effects of pumping are immediately observable, and may affect the associated streams' discharge rates. However, at the tested pumping rate of  $468 \text{ m}^3/\text{d}$ , the discharge decrease in terms of the Little Smoky River's overall discharge rates are relatively insignificant (Figure 21). This suggests that the bedrock aquifers within the study area could support water well pumping at rates similar to those tested.

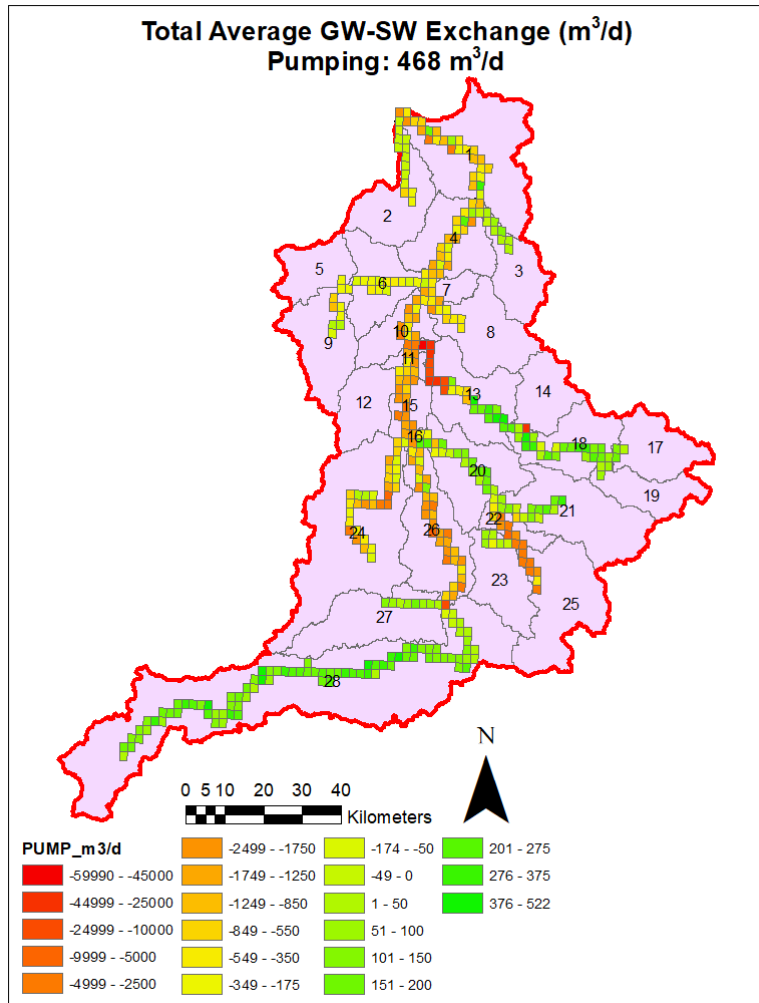


**Figure 21: Plan view map of the Little Smoky River watershed, with GW-SW exchanges displayed for each MODFLOW river grid cell. Pumping wells that have been installed within and proximal to the study area extract water at a rate of 468 m<sup>3</sup>/d, for six months of each simulation year.**

A climate change run over the 2010-2034 period was the next scenario to be applied. The coupled SWAT-MODFLOW model was run five separate times, each with a different GCM. The results of each run were then averaged to yield one harmonized output, with the GW-SW exchange rates shown in Figure 22A. Immediately noticeable in the figure is that the base scenario and the climate change scenario's GW-SW interaction patterns look similar. This is

indeed the case, as the overall average flow rate observed in the averaged climate change scenario is  $-1,294.14 \text{ m}^3/\text{d}$ , while that of the base scenario is  $-1,294.04 \text{ m}^3/\text{d}$  (both indicating overall discharge into the river). These results indicate that the effects of climate change on this watershed over the 2010-2034 period are negligible. A likely reason for the climate change scenario's lack of influence is that the simulation period was quite short in terms of overall climate trends, with little change occurring in the predicted  $\text{CO}_2$  concentration over this timespan for the RCP8.5 scenario, as well as all other scenarios ( $\sim 375$  to  $\sim 475$  ppm; see Figure 13).

As the most complex scenario to be tested in this study, the five coupled climate change scenarios were run again with a MODFLOW model that included the higher pumping rate of  $4680 \text{ m}^3/\text{d}$ . The effects of the elevated pumping rates caused a more distinct change in the GW-SW interaction pattern of the watershed for the 2010-2034 forecast. The substantial increase in the volume of pumped water may have left less stored GW in the study area's primary aquifers (i.e. the Paskapoo Fm.), as the discharge rates for each river cell are observed to decrease on average (Figure 22B). This storage trend can also be observed in the MODFLOW model before coupling, with model-wide fluxes from storage spiking to correspond with pumping intervals (from un-pumped totals of under  $1 \text{ m}^3/\text{d}$  up to total maximums of  $\sim 1,000,000 \text{ m}^3/\text{d}$ ). While the total average discharge into the rivers was  $1,294 \text{ m}^3/\text{d}$  in the initial SWAT-MODFLOW model (1983-2007), this average was reduced to  $1,174 \text{ m}^3/\text{d}$  after simulating with the RCP8.5 GCMs and the elevated pumping schedule, with cell-by-cell flowrate differences ranging from under  $5 \text{ m}^3/\text{d}$  to over  $3,000 \text{ m}^3/\text{d}$  (discharge decreasing in 320 of 405 river cells). A comparison of the change in aquifer discharge under the tested simulation scenarios, i.e. with pumping and without pumping, indicates that anthropogenic influence can have more immediate effects on the study's watershed than those of climate change, even at the lower rate of  $468 \text{ m}^3/\text{d}$ .

Although water well pumping simulations were the only human influence applied to this study, the change in GW-SW exchange was measurable on a regional scale. However, the environmental footprint in the study area will only grow when considering additional human sectors (including agriculture). The fact that the potential effects of these operations can now be quantified with respect to both GW and SW resources is a key benefit of using a coupled model.

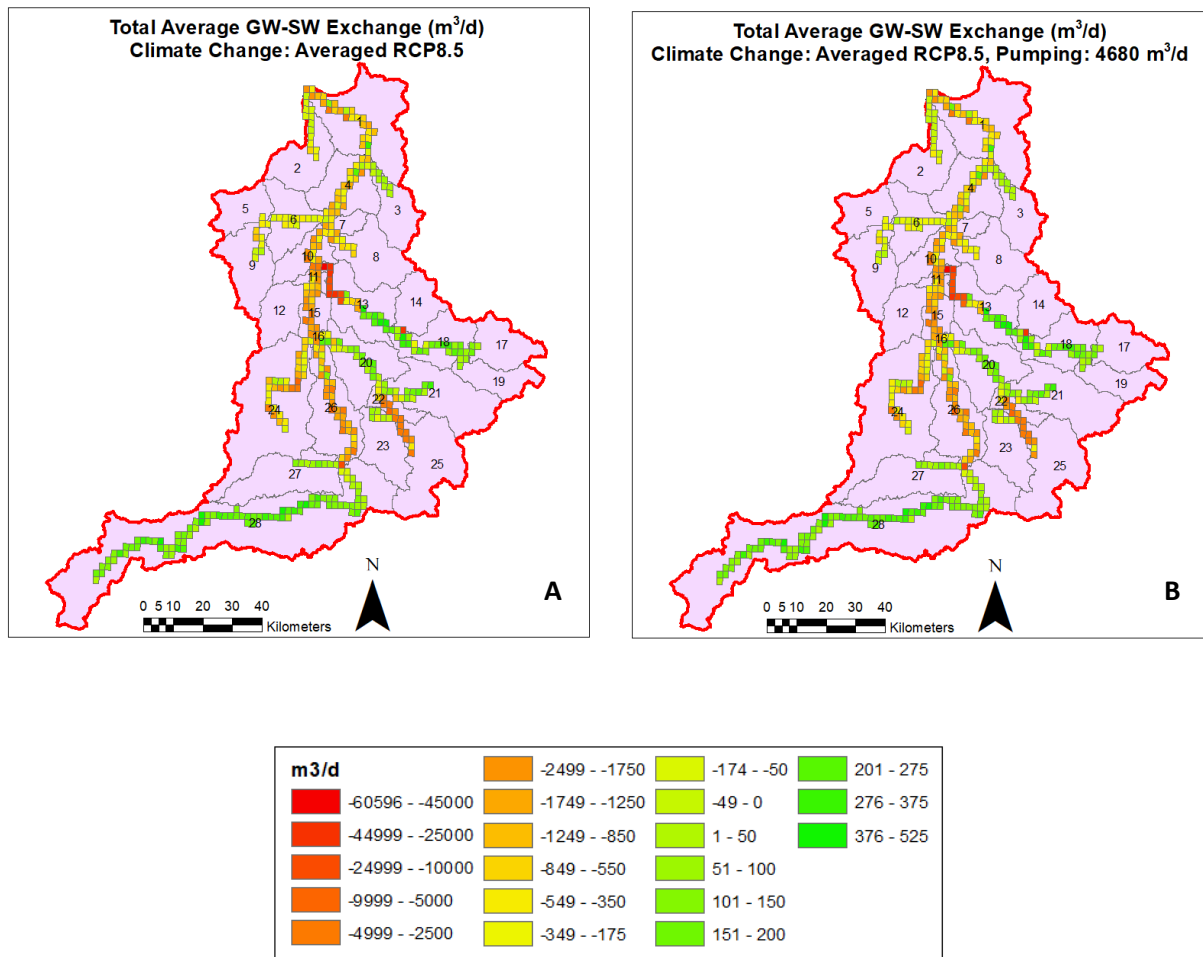


**Figure 22: Projected long-term (2010-2034) average annual GW-SW exchanges under two simulation scenarios. (A) solely shows the effects of climate change, and (B) also includes a water well pumping rate of 4680 m<sup>3</sup>/d (pumping wells are the same as in Figures 20 and 21).**

### **3.3. SWAT-MODFLOW as a GW-SW Tool**

#### *3.3.1. Watershed and Scenario Simulation*

SWAT-MODFLOW's ability to simulate the hydro(geo)logy of a watershed is fully dependent on the availability and quality of data, as well as the accuracy of its component models. Due to much time being spent on the calibration of both the SW and GW models, the coupled result proves to be robust in terms of its representation of river discharges (Figures 17A and B). Similar to the Sprague River model built by Bailey et al. (2016), high spatial variation in GW-SW exchange rates can be seen in each SWAT-MODFLOW figure in Section 3. The ability to gain information on these patterns may prove to be crucial for the informed management of both SW and GW resources in this watershed, as well as any other in which a SW-GW model has been applied.

Moreover, when additional stressors such as climate change and pumping simulations are included, it yields more information from a risk management perspective, especially when simulating worst-case scenarios such as that described in Section 3. Although only GCMs for RCP8.5 scenarios were used in this study, their use in the SWAT-MODFLOW simulations proved that this tool is capable of forecasting a wide range of outcomes, including any desired climate change data. Modellers can then choose, based on the scope and timeline of the project, how detailed of a model is suitable for management purposes. Based on the relatively fast run times observed in this study, much more finely discretized numerical models (including more local-scale river cells) using the same workflow are within reason for investigations with direct effects on watersheds, and are recommended for forecasting and/or risk assessment studies. In situations where operators are considering drilling programs in watersheds with a pronounced connection between the GW and SW systems, it is advised that these operators or the associated

regulatory bodies perform modelling exercises similar to that performed in this study in order to further understand the effects of either freshwater or GW extraction on a watershed.

### *3.3.2. Computational Time*

As mentioned in sections 2 and 3, the computational time required for a run of the first fully calibrated SWAT-MODFLOW model was roughly 6 hours – about half of the hypothesized run time. This run time was achieved on a machine with a Core i5. However, subsequent runs took approximately 4 hours, and were performed on a machine with 40 cores. Even faster run times are realistically possible on more powerful machines, or clouds with many processors. The four-hour run time of the coupled model on a 40-core machine is ideal for running multiple simulations per day, especially in studies where more than one scenario is to be analyzed (various data inputs, climate change scenarios, pumping, etc.). Including a pumping schedule in the coupled tool increases the total run time, with the amount of additional time being a factor of the complexity of the pumping schedule(s).

The run time of this model is shorter than that of Bailey et al. (2016) because the MODFLOW model's grid was more coarsely discretized. The 100 x 100 grid used here lacks the detailed definition found in other SWAT-MODFLOW models (Kim et al., 2008; Guzman et al., 2015; Bailey et al., 2016), but employing a finer grid on the geographic scale of this study's model, especially considering the relative complexity of this model's 7-layer subsurface representation, would have caused computational time to increase beyond what is reasonable. In addition, the purpose of this study was to test the SWAT-MODFLOW code under variable conditions, while most other studies have focused on producing a model to be used directly by policymakers.

### **3.4. Limitations**

#### *3.4.1. Limitations: SWAT*

The primary strength of the SWAT model is its ability to efficiently simulate large watersheds over extended study periods (Faramarzi et al., 2015; Bailey et al., 2016), but due to SWAT's calculations being divided into HRUs, SWAT can be hindered by its semi-distributed nature. When defining HRUs based on soil, land use and slope, one must be conscious of finding a balance between detail and computational efficiency. Although this information is scaled up to the subbasin level, this may present problems when certain subbasins contain many soil or land use types and can result in the model missing some information. This was not a major setback in this study, however, as the SWAT model had subbasins with soil and land use types that were fairly dominant in their areas, ensuring acceptable coverage of the watershed's characteristics. Further to the mechanics of HRUs, their lack of defined geo-locations is useful for obtaining variable data within a subbasin (Bailey et al., 2016). This comes with the downside of being unable to pinpoint where in the subbasin of interest any given piece of information may be for. While this gives a range of detailed data within a subbasin, actual visual representation of that data must still occur at the subbasin level itself.

#### *3.4.2. Limitations: MODFLOW*

Though reliable and heavily used in both academic and corporate/consulting environments, MODFLOW (specifically Visual MODFLOW Classic) is not without drawbacks. When constructing a MODFLOW model using the Classic interface, a rectangular grid is imposed in each of the three dimensions, which introduces difficulties when attempting to represent the real world. Sophocleous et al. (1999), when developing the first SWAT-MODFLOW model, noted

that MODFLOW's rectangular grid does not provide a perfect simulation for river or stream channels, which have a more rounded architecture. However, tests performed in the same study found that if the channel is significantly wider than it is deep (which is the case for most of the Little Smoky River), the observed flow patterns do not show much difference from those simulated by MODFLOW (Sophocleous et al., 1999).

Throughout the model, each of these rectangular grid cells remains intact. This means that even in areas where a pinching-out formation may exist (which would theoretically get rid of a grid cell), the cells' layout prevents the layer from fully disappearing. When this happens, a minimum thickness of 1 unit (defined when setting up the model; meters or feet) remains, creating what is effectively an infinitesimally thin area of the layer in question. If there are multiple layers like this stacked on top of one another, it can inhibit the simulated water from flowing through each layer, resulting in far higher hydraulic heads (differences of nearly 400 meters in some cases) than actually exist.

The workaround utilized in this study was simple: for areas with multiple stacked thin layers (primarily the northwest corner of the model), a minimum layer thickness of 50 meters was imposed. Hydraulic conductivities were then manually changed to correspond to the formations below, so as to imitate a pinching-out succession. Although this method does not completely eliminate the stacking-heads problem, hydraulic heads in problem areas were reduced by at least 100 meters. In addition, constant head boundary conditions based on observation wells were employed in this area of the model. When the model was run with both workaround conditions set, the root mean square error in hydraulic heads was reduced significantly (from ~36% to ~7.5% normalized root mean square error, further reduced to 6.25% at the end of calibration).

### 3.4.3. Limitations: SWAT-MODFLOW

If each component model is built and calibrated effectively, SWAT-MODFLOW acts as a powerful tool for simulating integrated GW-SW interaction. Although this has been established in the current study and those previously done (Sophocleous et al., 1999; Kim et al., 2008; Guzman et al., 2015; Bailey et al., 2016), the tool's current novelty and dependence on its components give rise to some limitations.

Firstly, a SWAT-MODFLOW model's performance is fully governed by the quality and refinement of its components. Therefore, in study areas that may be lacking in either SW- or GW-related inputs or observational data, the ability to produce a faithful model may be limited. In addition, this coupled tool encounters a limitation shared with all models: the trade-off between scientific accuracy and computational burden. One has the flexibility with SWAT-MODFLOW to discretize both of its component models to any desired refinement (Guzman et al., 2015; Bailey et al., 2016). However, the goals of the study (and lack of access to computational power/data) may limit the ability to produce models of such fine detail. In such cases, the limitations of SWAT and MODFLOW may, in fact, resurface.

Similarly, the calibration and uncertainty assessment processes followed for each component model will affect the performance of the SWAT-MODFLOW tool. This study's coupled model used the best simulation results for SWAT, and the final results of manual calibration for MODFLOW, which were deemed to be satisfactory for the purposes of this study. As these components are subject to non-uniqueness, studies using multiple calibration methods are an opportunity to address the coupled tool's model uncertainty.

The SW component of SWAT-MODFLOW, SWAT, is primarily used for regional studies of hydrology due to its efficient HRU-based computational scheme (Faramarzi et al., 2015; Bailey et al., 2016). Because of this, however, the ability of SWAT-MODFLOW to simulate site-specific processes may be limited. It is therefore important for an adequate model selection process to occur so that the goals of the study are met.

Study-specific limitations of the SWAT-MODFLOW model built include the fact that the component models were calibrated over a relatively brief period with respect to the overall hydro-climate. As this study's calibrated parameters reflect short-term dynamics over 25 years, large-scale temporal variations may not have been accounted for. In light of this, further studies are required to assess the robustness of this tool when subjected to a wider range of natural climate variability.

In addition to the above, the sheer volume of output data produced by the daily-time-step model may not suit all purposes. An example is the GW-SW exchange output file (swatmf\_out\_MF\_gsw), which provides flow data for every MODFLOW river grid cell, at each time step. Although this can be incredibly useful for very short-term studies (over the course of 0-5 years), it is seldom required for long-term regional flow models such as the one built in this study, whose desirable outputs often include total average fluxes, or average fluxes for specific months. As of now, this SWAT-MODFLOW code runs solely on a daily time step, even though the component models, as in this study, may not be built and/or calibrated as such. For longer-term projects, a weekly or monthly time step may be more suitable and would significantly reduce computational time of the coupled model.

### 3.5. Future Research Directions

A major goal of this study was to establish that the SWAT-MODFLOW code used by Bailey et al. (2016) could be applied to semi-arid regions with highly variable climate. Due to the study's success in this endeavor, this expands the uses of SWAT-MODFLOW to analyze GW-SW interactions in numerous other catchments in the world, including ones with widely fluctuating climate patterns. In particular, the methodology and workflow applied in this study can be used as an analogue for other semi-arid regions, especially those where water conflicts are becoming, or already are, prominent. Examples of this may include Saskatchewan, North Dakota and the Permian Basin. In addition, this modeling framework can be used to model regions of highly variable scale (local or regional, depending on the study's goals).

Possible avenues for future research in this study area include more detailed water well pumping simulations from bedrock aquifers. A more finely discretized SWAT-MODFLOW model (especially the MODFLOW component, at an optimal watershed scale) would be able to provide more insight into the effects of GW extraction on a region's SW resources. This will be particularly important for river grid cells, as the local refinement will result in more accurate GW-SW interaction patterns, yielding more reasonable values for exchange rates and drawdown. Having already been applied to shallow aquifers in the Musimcheon Basin of South Korea (Kim et al., 2008), performing such tests in the bedrock aquifers of a more geologically complex area would expand the uses this tool. Further studies in this area are especially viable in semi-arid regions such as Alberta, where GW extraction for hydraulic stimulation operations is becoming increasingly prevalent.

Another use of increasing importance is climate change simulation. Due to SWAT's ability to simulate various climate change scenarios, future coupled models may be able to increase the

understanding of how these changes will affect the GW system. Of high priority would be the best-case and worst-case scenarios with respect to CO<sub>2</sub> emissions (RCP 2.6 and 8.5) for the closest decades, which would shed light on how the management of water resources must change on a short-term basis. However, as the results of this study showed little change due to climate over the short-term, longer-term forecasting may be required to forecast overall trends. Since SWAT-MODFLOW also provides more detailed baseflow values in general, climate change simulations using a coupled model should theoretically be an improvement over SWAT models. To more completely assess the various demands within the WFE nexus, water conflicts between sectors will also be a growing area of study. As such, conducting research where the water extraction rates from the petroleum, agriculture and domestic sectors are all considered under various climate change scenarios will increase the ability of decision-makers to quantify the interrelated demands on water as a holistic GW-SW system.

#### **4. CONCLUSION**

It is becoming increasingly important to understand the interrelated nature of water resources, and to consider them in a unified manner. This is especially true in areas like Alberta, where significant demands are placed on these resources from multiple sectors. Hydro(geo)logic models can help us to forecast and visualize complex scenarios, as well as to make more informed decisions about the management of these resources. Coupled or integrated hydro(geo)logic models are one of scientists' best available tools for this purpose, as they track the interactions between both vital components in the hydrologic system.

This study tested the robustness of one such tool, SWAT-MODFLOW, in an area defined by its diversity in terms of its weather and hydrogeology. Although some fully integrated models may offer more in terms of faithful representation of the scientist's conceptual model (Sudicky et al., 2008), the code tested here performed successfully under highly variable hydro(geo)logic and weather conditions while incorporating a deeper, more complex bedrock system than any prior SWAT-MODFLOW model. The model also included additional factors such as snow influence that had not been included in previous SWAT-MODFLOW studies. The implementation of this SWAT-MODFLOW model proved that GW has a heavy influence on the hydrology of the Little Smoky River watershed, discharging significant volumes of water into the rivers and tributaries of the study area. This reinforces the importance of examining SW and GW as one system, as the demands placed on one have direct effects on the other.

The modeling framework developed here can be used to map GW-SW interaction on a finer scale than SWAT can by itself, with MODFLOW river grid cells providing multiple unique outputs within each SWAT subbasin, at any time step. In addition, the code used in this study (Bailey et al., 2016) is available, free of charge, to the public, which has the potential to save thousands of dollars on project budgets. Use of this tool can help scientists track water resources more accurately, and can inform the decisions made by policymakers whose priority is to ensure that this vital resource can remain available to all that need it.

## REFERENCES

- Abbaspour, K., 2015. User Manual for SWAT-CUP: SWAT Calibration and Uncertainty Analysis Programs, Eawag: *Swiss Fed. Inst. of Aquatic Science and Technology* [http://www.eawag.ch/organization/abteilungen/siam/software/swat/index\\_EN/](http://www.eawag.ch/organization/abteilungen/siam/software/swat/index_EN/).
- Alberta Agriculture and Forestry, 2018. Current and Historical Weather Station Data Viewer – Brought to you by the Alberta Climate Information Service (ACIS). URL: <https://agriculture.alberta.ca/acis/alberta-weather-data-viewer.jsp>
- Alberta Energy Regulator (AER) bulletin 2015-25: Restrictions to Temporary Diversion 368 Licences. URL: <https://www.aer.ca/documents/bulletins/Bulletin-2015-25.pdf>
- Alberta Geological Survey (AGS), 2015. Alberta Table of Formations. Alberta Energy Regulator. URL: <https://ags.aer.ca/document/Table-of-Formations.pdf>. Accessed on Sept 22, 2018.
- Alberta Water Portal Society, 2017. The history of climate in Alberta and effects of climate change on Alberta's watersheds. *History and effects of climate change on Alberta's watersheds*. URL: <https://albertawater.com/history-and-effects-of-climate-change-on-alberta-s-watersheds>
- Alessi, D. S., Zolfaghari, A., Kletke, S., Gehman, J., Allen, D. M., Goss, G. G., 2017. Comparative analysis on hydraulic fracturing wastewater practices in unconventional shale development: Water sourcing, treatment and disposal practices. *Canadian Water Resources Journal*, 42(2), 105-121.

- Arnold, J.G., Srinivasan, R., Muttiah, R.S., Williams, J.R., 1998. Large area hydrologic modeling and assessment Part 1: model development. *Journal of American Water Resource Association*, 34, 73-89. URL: <http://dx.doi.org/10.1111/j.1752-1688.1998.tb05961.x>.
- Arnold, J. G., Kiniry, J. R., Srinivasan, R., Williams, J. R., Haney, E. B., Neitsch, S. L., 2012. Soil & Water Assessment Tool – Input/Output Documentation, Version 2012. *Texas Water Resources Institute*, TR-439.
- Bachu, S., Michael, K., 2002. Hydrogeology and Stress Regime of the Upper Cretaceous-Tertiary Coal-Bearing Strata in Alberta. *Alberta Energy and Utilities Board*, EUB/AGS Earth Sciences Report 2002-04.
- Bailey, R. T., Wible, T. C., Arabi, M., Records, R. M., Ditty, J., 2016. Assessing regional-scale temporal patterns of groundwater-surface water interactions using a coupled SWAT-MODFLOW model. *Hydrological Processes*, 30, 4420-4433.
- Bailey, R. T., Rathjens, H., Bieger, K., Chaubey, I., Arnold, J. G., 2017a. SWATMOD-Prep: Graphical user interface for preparing coupled SWAT-MODFLOW simulations. *Journal of the American Water Resources Association*, JAWRA-15-0204-P.
- Bailey, R. T., 2017b. SWAT-MODFLOW Workshop. *Colorado State University*. Presentation.
- Beets, L., 2016. SWAT-MODFLOW Documentation. *Wageningen University & Research*. Word Document.
- Bizikova, L.; Roy, D.; Swanson, D.; Venema, H.D.; McCandless, M., 2013. The Water-Energy-Food Security Nexus: Towards a practical and decision-support framework for landscape

- investment and risk management. *International Institute for Sustainable Development*, Report. Available online: URL <https://www.iisd.org/library/water-energy-food-security-nexus-towards-practical-planning-and-decision-support-framework>.
- Brinsky, J., 2014. Basal Belly River Hydraulic Head and Show Map. *Encana Corporation*.
- Brunner, P., Simmons, C. T., 2012. HydroGeoSphere: a fully integrated, physically based hydrological model. *Groundwater*, 50(2), 170-176.
- Campbell, C., 2015. Little Smoky – Duvernay Pilot: How Close is Promised Cumulative Effects Management? *WLA*, Volume 23, No. 5, 11-13.
- Cannon, A. J. Selecting GCM Scenarios that Span the Range of Changes in a Multimodel Ensemble: Application to CMIP5 Climate Extremes Indices. *J. Climate* **2015**, 28(3), 1260-1267. DOI: <https://doi.org/10.1175/JCLI-D-14-00636.1>
- Chen, J., Brissette, F. P., Leconte, R., 2011. Uncertainty of downscaling method in quantifying the impact of climate change on hydrology. *J. Hydrol.*, 401, 190-202. DOI: <https://doi.org/10.1016/j.jhydrol.2011.02.020>
- Chevron Canada. 2017. *Our History in Fox Creek*. URL: <http://www.chevron.ca/our-businesses/kaybob-duvernay-appraisal-program/our-history-in-fox-creek>
- Ely, D. M., Kahle, S. C., 2012. Simulation of Groundwater and Surface-Water Resources and Evaluation of Water-Management Alternatives for the Chamokane Creek Basin, Stevens County, Washington. *U.S. Department of the Interior, U.S. Geological Survey, Scientific Investigations Report 2012-5224*, 86pp.

- Faramarzi, M., Srinivasan, R., Iravani, M., Bladon, K. D., Abbaspour, K. C., Zehnder, A. J. B., Goss, G. G., 2015. Setting up a hydrological model of Alberta: Data discrimination analyses prior to calibration. *Environmental Modelling and Software*, 74, 48-65.
- Faramarzi, M., Abbaspour, K., Adamowicz, W.L., Lu, W., Fennell, J., Zehnder, A.J.B, Goss, G., 2017. Uncertainty based assessment of dynamic freshwater scarcity in semi-arid watersheds of Alberta, Canada, *Journal of Hydrology: Regional Studies*, 9, 48-68.
- Farvolden, R. N., 1961. Groundwater resources, Pembina area, Alberta. *Research Council of Alberta*, 61-4, 26pp.
- Food and Agriculture Organization (FAO), 1995. The Digital Soil Map of the World and Derived Soil Properties. CD-ROM, Version 3.5, Rome.
- Government of Canada, 2015. Canadian Land Cover, circa 2000 (Vector) – GeoBase Series – ARCHIVED. URL: <https://open.canada.ca/data/en/dataset/97126362-5a85-4fe0-9dc2-915464cfd7bb7>
- Government of Canada, 2017. Soil Landscapes of Canada (SLC). URL: <http://sis.agr.gc.ca/cansis/nsdb/slc/index.html>
- Grasby, S., Tan, W., Chen, Z., and Hamblin, A.P. 2007. Paskapoo groundwater study. Part I: Hydrogeological properties of the Paskapoo Formation determined from six continuous cores. *Geological Survey of Canada*, Open File 5392, 6pp.
- Grasby, S.E., Chen, Z., Hamblin, A.P., Wozniak, P.R.J. and Sweet, A.R. 2008. Regional characterization of the Paskapoo bedrock aquifer system, southern Alberta. *Canadian Journal of Earth Sciences*, 45(12): 1501–1516.

- Guzman, J. A., Moriasi, D. N., Chu, M. L., Starks, P. J., Steiner, J. L., Gowda, P. H., 2013. A tool for mapping and spatio-temporal analysis of hydrological data. *Environmental Modelling & Software*, Volume 48, 163-170.
- Guzman, J. A., Moriasi, D. N., Gowda, P. H., Steiner, J. L., Starks, P. J., Arnold, J. G., Srinivasan, R., 2015. A model integration framework for linking SWAT and MODFLOW. *Environmental Modelling & Software*, Volume 73, 103-116.
- Hamblin, A.P. 2004. Paskapoo-Porcupine Hills Formations in western Alberta: synthesis of regional geology and resource potential. *Geological Survey of Canada*, Open File 4679, 30pp.
- Horlemann, L., Neubert, S., 2006. Virtual water trade: a realistic concept for resolving the water crisis? *Rep. 25*, German Dev. Inst., Bonn, Germany.
- Hoff, H., 2011. Understanding the nexus (Background paper for the Bonn2011 Nexus Conference).
- Hughes, A. T., Smerdon, B. D., Alessi, D. S., 2017. Hydraulic properties of the Paskapoo Formation in west-central Alberta. *Canadian Journal of Earth Sciences*, 54(8), 883-892. <https://doi.org/10.1139/cjes-2016-0164>
- Hyndman, R. J., Koehler, A. B., 2006. Another look at measures of forecast accuracy. *International Journal of Forecasting*, 22(4), 679-688.
- IPCC, 2014. Climate Change 2014: Synthesis Report. Contribution of Working Groups I, II and III to the Fifth Assessment Report of the International Panel on Climate Change [Core

- Writing Team, R. K. Pachauri and L. A. Meyer (eds.)]. *IPCC*, Geneva, Switzerland, 151pp.
- Jarvis, A., Reuter, H. I., Nelson, A., Guevara, E., 2008. Hole-filled SRTM for the Globe Version 4, the CGIAR-CSI SRTM 90m Database. URL: <http://srtm.csi.cgiar.org>
- Johnson, E. G., Johnson, L. A., 2012. Hydraulic Fracture Water Usage in Northeast British Columbia: Locations, Volumes and Trends. *B.C. Ministry of Energy and Mines, Geoscience Reports 2012*, 41-63.
- Kim, N. W., Chung, I. M., Won, Y. S., 2004a. The development of fully coupled SWAT-MODFLOW model (I) model development. *J. Korea Water Resour. Assoc.* 37(6), 503-512.
- Kim, N. W., Chung, I. M., Won, Y. S., 2004b. The development of fully coupled SWAT-MODFLOW model (II) evaluation of model. *J. Korea Water Resour. Assoc.* 37(6), 513-521.
- Kim, N. W., Chung, I. M., Won, Y. S., Arnold, J. G., 2008. Development and application of the integrated SWAT-MODFLOW model. *Journal of Hydrology (2008)*, 356, 1-16.
- Knapik, L. J., Lindsay, J. D., 1983. Reconnaissance Soil Survey of the Iosegun Lake Area, Alberta. *Alberta Research Council, Bulletin 43*, 100pp.
- Leavesley, G. H., Lichty, R. W., Troutman, B. M., Saindon, L. G., 1983. Precipitation-runoff modeling system – User’s manual. *U.S. Geological Survey Water-Resources Investigations Report 83-4238*, 207pp.

- Markstrom, S. L., Niswonger, R. G., Regan, R. S., Prudic, D. E., Barlow, P. M., 2008. GSFLOW – Coupled Ground-Water and Surface-Water Flow Model Based on the Integration of the Precipitation-Runoff Modeling System (PRMS) and the Modular Ground-Water Flow Model (MODFLOW-2005). *U.S. Geological Survey, Techniques and Methods 6-D1*, 254pp.
- Masud, M. B., McAllister, T., Cordeiro, M. R. C., Faramarzi, M., 2018. Modeling future water footprint of barley production in Alberta, Canada: Implications for water use and yields to 2064. *Science of the Total Environment 616-617(2018)*, 208-222.
- McDonald, M. G., Harbaugh, A. W., 1983. A modular three-dimensional finite-difference ground-water flow model. *US Geological Survey, USGS Open-File Report 83-875*.
- Neitsch, S. L., Arnold, J. G., Kiniry, J. R., Williams, J. R., 2009. Soil and Water Assessment Tool – Theoretical Documentation, Version 2009. *Texas Water Resources Institute, TR-406*.
- Niswonger, R. G., Panday, S., Ibaraki, M., 2011. MODFLOW-NWT, A Newton formulation for MODFLOW-2005. *U.S. Geological Survey Techniques and Methods 6-A37*, 44pp.
- Notte, C., Allen, D. M., Gehman, J., Alessi, D. S., Goss, G. G., 2017. Comparative analysis of hydraulic fracturing wastewater practices in unconventional shale development: Regulatory and policy regimes. *Canadian Water Resources Journal*, 42(2): 122-137.
- Pacific Climate Impacts Consortium, 2014. Statistically Downscaled Climate Change Scenarios. Available online: URL <https://www.pacificclimate.org/data/statistically-downscaled-climate-scenarios> (accessed 25 June, 2018).

- Park, S., Bailey, R. T., 2017. SWAT-MODFLOW Tutorial – Documentation for preparing model simulations. Department of Civil and Environmental Engineering, Colorado State University, 56pp.
- Paktinat, J., O’Neill, B., Tulissi, M., 2011. Case studies: impact of high salt tolerant friction reducers on fresh water conservation in Canadian shale fracturing treatments. *Society of Petroleum Engineers, Conventional Unconventional Resources Conference*, November 15-17, 2011.
- Pearson, K., 1895. Notes on regression and inheritance in the case of two parents. *Proceeding of the Royal Society of London*, Volume 58, 240-242.
- Petrel Robertson Consulting Ltd., 2014. Integrated assessment of water resources for unconventional oil and gas plays, west-central Alberta: aquifers in shallow bedrock and surficial sediments, final (year 2) report. *Petroleum Technology Alliance of Canada*, 32pp.
- Sauchyn, D., 2017. Climate Variability and Change in the Athabasca River Basin. *Alberta WaterSMART*. URL: <http://albertawatersmart.com/featured-projects/collaborative-watershed-management.html>
- Scanlon, B. R., Reedy, R. C., Male, F., Hove, M., 2016. Managing the Increasing Water Footprint of Hydraulic Fracturing in the Bakken Play, United States. *Environ. Sci. Technol.* 50 (18), 10273-10281.
- Schindler, D. W., Donahue, W. F., 2006. An impending water crisis in Canada’s western prairie provinces. *Proceedings of the National Academy of Sciences of the United States of America*, 103 no. 19, 7210-7216.

- Smerdon, B. D., Atkinson, L., Hughes, A. T., 2016. Aligning Groundwater Mapping with the Scale of Regulation in the Fox Creek Area. *WaterTech*, AGS-04-07-16.
- Sophocleous, M. A., Koelliker, J. K., Govindaraju, R. S., Birdie, T., Ramireddygari, S. R., Perkins, S. P., 1999. Integrated numerical modeling for basin-wide water management: The case of the Rattlesnake Creek basin in south-central Kansas. *Journal of Hydrology*, Volume 214, Issue 1, p. 179-196.
- St. Jacques, J-M., Sauchyn, D. J., Zhao, Y., 2010. Northern Rocky Mountain streamflow records: Global warming trends, human impacts or natural variability? *Geophysical Research Letters - Hydrology and Land Surface Studies*, Volume 37, Issue 6, L06407.
- Sudicky, E. A., Jones, J. P., Park, Y. J., Brookfield, A. E., Colautti, D., 2008. Simulating complex flow and transport dynamics in an integrated surface-subsurface modeling framework. *Geosciences Journal*, 12(2), 107-122.
- Texas A & M, 2017. SWAT: Soil & Water Assessment Tool. URL: <http://swat.tamu.edu/>
- Therrien, R., 1992. Three-dimensional analysis of variably-saturated flow and solute transport in discretely-fractured porous media. Ph.D. thesis, University of Waterloo, Waterloo, ON.
- Tóth, J., 1963. A theoretical analysis of groundwater flow in small drainage basins. *Journal of Geophysical Research*, 68 no. 16, 4795-4812.
- van der Gun, J., 2012. Groundwater and Global Change: Trends, Opportunities and Challenges. *United Nations World Water Assessment Programme: Side Publications Series*, 01, WWDR4, 44pp.

van Vuuren, D. P., Edmonds, J., Kainuma, M., Riahi, K., Thomson, A., Hibbard, K., Hurtt, G. C., Kram, T., Frey, V., Lamarque, J-F., Masui, T., Meinshausen, M., Nakicenovic, N., Smith, S. J., Rose, S. K., 2011. The representative concentration pathways: an overview. *Climatic Change*, 109:5. <https://doi.org/10.1007/s10584-011-0148-z>

The Weather Network, 2018. Statistics: Fox Creek, Alberta. URL:

<https://www.theweathernetwork.com/ca/api/sitewrapper/index?b=%2Fstatistics%2F&p=%2Fforecasts%2Fstatistics%2Findex&url=%2Fstatistics%2Fcaab0127%2Ffox-creek%2F%2F%2F%3F>

Wright, G.N. (ed.) 1984. The Western Canada Sedimentary Basin, a series of geological sections illustrating basin stratigraphy and structure. *Calgary, Canadian Society of Petroleum Geologists and the Geological Association of Canada.*

Yang, H., Zehnder, A., 2007. “Virtual water”: An unfolding concept in integrated water resources management. *Water Resources Research*, Volume 43, W12301.

## APPENDIX

**Table A1: List of major developments in SWAT-MODFLOW use, with alternative tools listed below.**

<b>SWAT-MODFLOW Models</b>			
<b>Year</b>	<b>Author</b>	<b>Title</b>	<b>Key Developments</b>
1999	Sophocleous et al.	Integrated numerical modeling for basin-wide water management: The case of the Rattlesnake Creek basin in south-central Kansas	First fully coupled SWAT-MODFLOW model to be applied to a watershed
2008	Kim et al.	Development and application of the integrated SWAT-MODFLOW model	First published SWAT-MODFLOW model to include a detailed water well pumping schedule
2015	Guzman et al.	A model integration framework for linking SWAT and MODFLOW	First SWAT-MODFLOW model to have simultaneously built component models (using SWATmf-app)
2016	Bailey et al.	Assessing regional-scale temporal patterns of groundwater-surface water interactions using a coupled SWAT-MODFLOW model	First SWAT-MODFLOW code to be endorsed by SWAT, and publicly available on the SWAT website
<b>Other Available GW-SW Models</b>			
<b>Year</b>	<b>Author and Model Name</b>	<b>Title</b>	<b>Key Developments</b>
2008	Sudicky et al.: HydroGeoSphere	Simulating complex flow and transport dynamics in an integrated surface-subsurface modeling framework	Most powerful GW-SW tool currently available
2008	Markstrom et al.: GSFLOW	GSFLOW – Coupled Ground-Water and Surface-Water Flow Model Based on the Integration of the Precipitation-Runoff Modeling System (PRMS) and the Modular Ground-Water Flow Model (MODFLOW-2005).	GW-SW model developed by USGS. Direct competitor with SWAT-MODFLOW

**Table A2: Data sources for the study's SWAT and MODFLOW component models.**

Data Sources for SWAT Model		Dataset	Resolution/Coverage	Time Span	Time Step	Region	Reference
Type							
Climate	Meteorological Stations	N/A		1983-2007	Daily	Local	Faramarzi et al., 2015
	Streamflow	2 in Study Area		1986-2007	Daily (monthly calibration)	Local	<a href="http://www.ec.gc.ca/rhc-wsc/">http://www.ec.gc.ca/rhc-wsc/</a>
	Digital Elevation Map	30 m * 30 m		N/A	N/A	Provincial	(Jarvis et al., 2008) <a href="http://www.geobase.ca/geobase/en/data/landcover/csc2000v/description.html">http://www.geobase.ca/geobase/en/data/landcover/csc2000v/description.html</a>
Digital Maps	Land Use Map	13 Feature Classes		1983-2007	N/A	Local	<a href="http://sis.agr.gc.ca/cansis/nsdb/sl/index.html">http://sis.agr.gc.ca/cansis/nsdb/sl/index.html</a>
	Soil Map	20 Feature Classes		1983-2007	N/A	Local	
Climate Change Data	Precipitation		300 arc sec	2010-2034	Daily	Downscaled to Local	Pacific Climate Impacts Consortium (PCTC) Cannon et al., 2015
	Temperature		300 arc sec	2010-2034	Daily	Downscaled to Local	Pacific Climate Impacts Consortium (PCTC) Cannon et al., 2015
Data Sources for MODFLOW Model		Dataset	Resolution/Coverage	Time Span	Time Step	Region	Reference
Type							
Elevation	Bedrock Formations - South	1 km * 1 km		N/A	N/A	Local	Alberta Geological Survey
	Bedrock Formations - North	Picked Fm. tops. 20 wells.		N/A	N/A	Local	AecuMap
Bedrock Properties	Hydraulic Conductivity, Specific Storage	1 km * 1 km		N/A	N/A	Local	Alberta Geological Survey
	Constant Head	N/A		1983-2007	Constant	Provincial	(Brinsky, 2014), SWAT Output
	Rivers	405 Grid Cells		1983-2007	Constant	Local	SWAT Output
Boundary Conditions	Recharge	Subbasin-scale		1986-2007	Monthly	Local	SWAT Output
	Streamflow	2 in Study Area		1986-2007	Daily (monthly calibration)	Local	<a href="http://www.ec.gc.ca/rhc-wsc/">http://www.ec.gc.ca/rhc-wsc/</a>
Observation Wells/Gauges	Legacy Borehole Data	377 in Study Area		2002-2007	Sporadic	Local	Alberta Geological Survey
Pumping Wells	Pumping Rate from Encana Well. Self-placed in model.	21 in Study Area		Days 1101-9131 of MODFLOW Simulation	Semi-yearly	Local	Encana Corporation

**Workflow A1: Complete process of exporting river data from a SWAT model to create a .RIV boundary for a MODFLOW model.**

1. Export MODFLOW's grid, and import it into SWAT as a shapefile.
2. Geo-reference the grid (was done manually in this study) to overlap with the study area's watershed.
3. Right click the MODFLOW grid shapefile, select "Joins and Relates," and then "Join".
4. Select "Join data from another layer based on spatial location."
5. Choose the point feature class as the joining layer.
6. Choose the second option: Each polygon will be given all the attributes of the line that is closest to its boundary, and the result will be a joint layer. The distance field (last one in the attribute table) shows how close the line is to each cell. Therefore, a line falling inside a polygon is treated as being closest to the polygon (i.e., a distance of 0).
7. Select the cells you are interested in by filtering based on the "Distance" field.
8. Export the selected cells.

**Workflow A2: Complete process of creating a .RCH file from the output of a SWAT model to import into the project's MODFLOW model.**

1. Open the "output.hru" file for the study's calibrated SWAT model in excel.
2. Perform the Text to Columns operation if necessary (to separate data by column).
3. Delete all columns except "HRU," "SUB," "MON," and "GW\_RCHGmm." This will yield a spreadsheet with monthly GW recharge values for the entire simulation period.
4. Delete the yearly average rows in each column.

5. Create two columns for Time 1 (T1) and Time 2 (T2), with the initial MODFLOW day in T1 and the final MODFLOW day in T2 for each monthly stress period. Add rows until the ending day of simulation. Repeat for each subbasin.
6. Organize columns in the following format:

```

File Edit Format View Help
30 1 Index 1 Subbasin_1
265 rchr entries
30 28.685          0          1101 1 2.55161e-313
30 1.646          1101          1132 1 0
30 0.57           1132          1160 1 0
30 0.245          1160          1191 1 0
30 26.585         1191          1221 1 0
30 14.931         1221          1252 1 0
30 5.393          1252          1282 1 0
30 2.089          1282          1313 1 0
30 0.768          1313          1344 1 0

```

Add rows as necessary for additional data, repeat for each subbasin. Left number will increase for next subbasin (31 instead of 30).

7. Insert the spreadsheet into the middle of MODFLOW's VMP file.

**Table A3: Weather gauges near the Little Smoky River watershed, with example average humidity and wind speed data for 2018 (modified from Alberta Agriculture and Forestry, 2018).**

Station Name	Date	Avg. Humidity (%)	Avg. Wind Speed (km/h)
Pass Creek Auto	Jan-18	81.216	14.408
Pass Creek Auto	Feb-18	74.663	15.504
Pass Creek Auto	Mar-18	75.862	13.368
Pass Creek Auto	Apr-18	60.831	13.703
Pass Creek Auto	May-18	55.098	13.886
Fox Creek Auto	Jan-18	91.742	5.351
Fox Creek Auto	Feb-18	85.69	7.517
Fox Creek Auto	Mar-18	83.403	6.156
Fox Creek Auto	Apr-18	68.481	7.047
Fox Creek Auto	May-18	60.418	5.788
Valleyview AGDM	Jan-18	80.788	13.637
Valleyview AGDM	Feb-18	73.689	14.826
Valleyview AGDM	Mar-18	73.701	13.008
Valleyview AGDM	Apr-18	64.145	14.121
Valleyview AGDM	May-18	51.202	14.368

Tony Auto	Jan-18	79.896	9.475
Tony Auto	Feb-18	73.379	10.158
Tony Auto	Mar-18	73.376	9.599
Tony Auto	Apr-18	58.563	10.172
Tony Auto	May-18	53.644	9.312
Berland Hills Auto	Jan-18	77.735	5.273
Berland Hills Auto	Feb-18	66.339	7.704
Berland Hills Auto	Mar-18	70.743	7.092
Berland Hills Auto	Apr-18	59.774	8.02
Berland Hills Auto	May-18	59.223	7.958

**Table A4: List of definitions for all parameters used in the SWAT-CUP calibration process (definitions based on Abbaspour, 2015). “sno” parameters are only applied to sub-basin 24. All other parameters were repeated with unique values for sub-basin 24. “v” denotes exact values, whereas “r” denotes relative changes to the parameter’s value. The “—” in some cells indicates that no value was used.**

Parameter	Definition	Initial	Final	Final (sub 24)
v PLAPS.sub	Precipitation change with increased elevation (mm H2O/km).	--	4.85	--
v TLAPS.sub	Temperature change with increased elevation (degrees C/km).	--	-13.65	--
v TMPINC().sub	Max/min temperature adjustment (degrees C)	--	-0.01575	-0.25925
r CN2.mgt	SCS curve number (function of soil permeability)	0.3	-0.20125	-0.44985
r ALPHA_BF.gw	Baseflow alpha factor. Gauges groundwater response to recharge changes (1/days)	0.1	0.1405	0.312
v REVAPMN.gw	Threshold water depth in shallow aquifer required for deep percolation to occur (mm H2O)	487.5	238.75	852.575012
v GW_DELAY.gw	Estimate for delay time	312.5	0.158225 (r)	1.7115

r	GW_REVAP.gw	Transfer rate between shallow aquifer and root zone, ranging from 0.02 (restricted) to 0.20 (unrestricted).	0.1505	0.022488	0.023858
v	GWQMN.gw	Threshold water depth in shallow aquifer required for return flow to occur (mm H2O)	1875	0.195 (r)	343.75
v	RCHRG_DP.gw	Fraction of deep water percolation from root zone (0.0 to 1.0)	0.475	0.124325 (r)	0.147938
v	CH_N2.rte	Manning's roughness coefficient ("n") for a channel (0.025 to 0.150)	0.18375	0.005 (r)	0.09875
v	CH_K2.rte	Effective hydraulic conductivity of the channel walls (mm/hr)	12.49025	0.0475	0.00325
v	ESCO.hru	Compensation factor for soil evaporation ranging from 0.01 (more evaporative demand from deeper soils) to 1 (less deep evaporative extraction)	0.325	0.791125	0.785125
v	EPCO.hru	Compensation factor for plant uptake ranging from 0.01 (less water uptake from deeper soil) to 1 (more water uptake from deeper soil)	0.725	0.827	0.75125
r	OV_N.hru	Manning's roughness coefficient ("n") for overland flow (0.010 to 0.480)	-0.38	-0.075	0.2275
v	HRU_SLP.hru	Average slope steepness (y/x, or m/m).	--	0.32625	0.0625
v	SLSUBBSN.hru	Average slope length (m), measured at the point that flow starts to concentrate. Generally no more than 90 m.	--	66.449997	31.4
v	SOL_AWC().sol	Soil layer's available water capacity (mm H2O/mm soil)	0.18	0.233	0.363425
r	SOL_K().sol	Soil's saturated hydraulic conductivity (mm/hr)	-0.22	-0.16465	-0.137675
r	SOL_BD().sol	Soil's moist bulk density (g/cm3 or Mg/m3). Generally between 1.1 and 1.9 g/cm3	-0.3	-0.08575	-0.00035

r SOL_ALB().sol	Soil's albedo (moist). Ratio of sunlight reflected to sunlight that hits the soil.	0.06	-0.125	0.095
v SUB_SFTMP().sno	Average temperature at which snowfall occurs (degrees C)	-19	--	-0.2425
v SUB_SMTMP().sno	Threshold temperature for snow melt to occur (degrees C)	3	--	0.9315
r SUB_SMFMX().sno	Snow melt factor on June 21 (mm H2O/degrees C - day)	-0.14	--	-0.135
r SUB_SMFMN().sno	Snow melt factor on December 21 (mm H2O/degrees C - day)	-0.14	--	0.055
v SUB_TIMP().sno	Lag factor of the snow pack's temperature (influenced by previous day's snow pack temperature)	0.425	--	0.135322